Boundary tracking control of flexible beams for transferring motions

K. D. Do

Department of Mechanical Engineering, Curtin University, Bentley, WA 6102, Australia
Email: duc@curtin.edu.au

Although flexible beams for transmitting both translational and rotational large motions are used in practice such as ocean drill pipes, their control has not been considered. This paper develops boundary feedback controllers to stabilize these beams at their reference configurations. Exact nonlinear partial differential equations governing motion of the beams in three-dimensional space are derived and used in the control design. The designed controllers guarantee globally practically asymptotically stability of the beam mo-tions at the reference states (i.e., positions and rotations of a straight beam moving axially with a desired velocity and rotating around its axial axis with a desired velocity). In the control design and analysis of well-posedness and stability, we utilize different transformations between the earth-fixed and body-fixed coordinates, Sobolev embeddings, and a Lyapunov-type theorem developed for a class of evolution systems in Hilbert space. Simulation results are also included to illustrate the effectiveness of the proposed control design.

Keywords: Beams; Transferring motions; Three dimensions; Large motions; Boundary control; Hilbert space; Evolution system.

1. Introduction

Beams for transferring axial linear and rotational motions are often encountered in practice. Typical examples are long drilling pipes and spindles, see Dong and Chen (2016) for a review on applications of drilling pipes in oil and gas industry. Due to the linear and rotational motions being transferred, the energy of the beams does not conserve. This makes sense because the beams need to transfer the desired energy. This is somewhat different from usual "non-moving" (stationary at the reference configuration) Bernoulli and Timoshenko beams. The transferred motions, slenderness, external loads, and nonlinear couplings between translational and rotational dynamics cause excessive large motions and vibrations. Thus, beams for transferring motions are necessarily controlled to reduce their large motions and vibrations. Boundary control of beams is an attractive and practical approach in comparison with distributed control because it only requires measurements and actuators implemented at their boundaries (usually at only one end) instead of distributed measurements and actuators as in distributed control, see Do and Pan (2008) for detailed discussion.

Boundary control of stationary (or "non-moving") Bernoulli and Timoshenko beams has received extensive attention from control community and excellent results have been achieved. Control of both large motions and vibrations of Bernoulli beams was considered (e.g., Do (2017a, 2017d, 2018b); Do and Pan (2008); He, Huang, and Li (2017); He, Meng, He, and Ge (2018); He, Nie, and Meng (2017) on boundary control of Bernoulli beams with small motions; Do (2017b, 2017c); Do and Lucey (2017, 2018); Do and Pan (2009) on boundary control of slender beams with large motions). For Timoshenko beams, most existing works focused on boundary control on their vibrations, see for example Endo, Matsuno, and Jia (2017); He, Ge, and C.Liu (2014); He, Meng, Liu, and Qin (2015); Kim and Renardy (1987); Manjunath and Bandyopadhyay (2009); Mei (2009); Morgul (1992); Queiroz, Dawson, Nagarkatti, and Zhang (2000); Xu and Wang (2013) based on Lyapunov's direct method or Krstic, Siranosian, and Smyshlyaev (2006); Krstic, Siranosian, Smyshlyaev, and Bement (2006) based on the backstepping method Krstic and Smyshlyaev (2008)). Boundary control of large motions of two- and three-dimensional Timoshenko beams was recently addressed in Do (2017e) and Do (2018c), respectively. The problem of controlling moving beams/strings was also addressed, see for example He, Nie, and Meng (2017); Yang, Hong, and Matsuno (2005) on boundary control of transverse motions of axially moving Bernoulli beams (see also Tabarrok, Leech, and Kim (1974) for dynamics of these beams), Tucker and Wang (2003) on control of torsional vibrations, Liu, Zhao, and He (2016a, 2016b, 2017) on stabilization of axially moving strings by boundary feedbacks. In these works (i.e., He, Nie, and Meng (2017); Liu et al. (2016a, 2016b, 2017); Tabarrok et al. (1974); Yang et al. (2005)), small motions (vibrations) are considered.

Boundary control and analysis of well-posedness and stability of moving beams governed by exact nonlinear partial differential equations (PDEs) have not been considered either in two- or three-

dimensional space. In practice, long beams for transferring axial and rotational motions such as ocean drill pipes can exhibit large motions. Strong nonlinear couplings between translational and rotational dynamics of these beams under large motions might result in a sudden failure. An example is the problem of loop formation due to couplings of the twisting and transverse motions.

This paper develops a new method to design boundary controllers for flexible beams in three-dimensional space for transferring axial and rotational motions under external loads. The beam under consideration is connected to an actuation system at one end, while the other end is connected to an object (e.g., drill head) that requires to be transferred axial and rotational motions. Exact nonlinear PDEs governing motions of the beam are derived and used in control design and analysis of well-posedness and stability. These require the unit quaternion for attitude representation, attitude tracking, Lyapunov's direct method, various Young's and Hölder's inequalities, Sobolev embedding, proper combinations of Earth-fixed and body-fixed coordinates, and cross vector products. Moreover, a Lyapunov-type theorem recently developed for study of well-posedness and stability analysis for a class of nonlinear evolution systems in Hilbert space is also used. The above tools are carefully utilized in conjunction with an introduction of a new Lyapunov functional for solving the tracking problem for beams.

The present paper covers the works in Do (2017c) and Do and Lucey (2018) but not vice versa, and is significantly advanced in comparison with the works in Do (2017c); Do and Lucey (2018), where a boundary control law was designed to stabilize both translational and rotational large motions of stationary flexible beams under deterministic and stochastic loads, respectively, due to the following three main reasons.

First, the configuration is different i.e., one end of the beam considered in Do (2017c); Do and Lucey (2018) is connected a fixed base via a ball-joint/fixed-joint. This eases the boundary control design at the other end because Sobolev embedding is not required to be used for deriving the relationship between motions of the fixed end to the motions of the whole beam. In other words, the boundary control at the actuated end does not need to stabilize motions of the fixed end. In the present paper, the uncontrolled end is connected to an object, which is free to move, for aforementioned applications. This significantly complicates the design of a boundary control at the actuated end and requires new tools from Sobolev embedding, see inequalities 6)-10) of Lemma 3.1.

Second, the reference configuration in Do (2017c); Do and Lucey (2018) is stationary while the reference configuration in the present paper moves axially and rotates around its axial axis for transmitting linear and rotating motions, i.e., the present paper considers velocity tracking problem while the work in Do (2017c); Do and Lucey (2018) addressed the stabilization objective. This together with the free-end configuration requires a new Lyapunov function (comparing (36) with (38) in Do (2017c) and (40) in Do and Lucey (2018)). The velocity tracking control problem for beams with both translational and rotational large motions is much harder than a stabilization one due to strong couplings among velocities, positions, attitudes, and deformations. This can be easily seen from the equations of motion (11) that if one component of the linear velocity vector and/or one compo-nent of the angular velocity vector is nonzero (i.e., tracking its reference value), all the other terms (positions, attitudes, remaining components of veoclity vectors) are potentially destabilized if no ap-propriate boundary controls are applied. The aforementioned couplings make the whole control design process much more involved than the one in Do (2017c) (comparing Section 4.2 with Section 5 in Do (2017c)) and Subsection 5.2 in Do and Lucey (2018) (removing the Hessian terms) when calculating the infinitesimal generator of Lyapunov functions.

Third, in Do (2017c); Do and Lucey (2018) and elsewhere the pitch angle, i.e. θ_2 in Subsection 2.1, is limited in the range $(-\frac{\pi}{2}, \frac{\pi}{2})$ because the Euler-angles are used to represent the attitude of the beam. The present paper overcomes this limitation by utilizing the quaternion vector to represent the attitude of the beam. The use of the quaternion vector allows the beam to operate in the whole three-dimensional space, and thus to cover a larger range of applications. Note that the quaternion vector is only used in simulations in Do (2017c) but not in the control design.

The rest of the paper is organized as follows: Equations of motion of the beam in space are briefly derived in Section 2; the control objective is formulated in Section 3; the control design is presented in Section 4.2, where the well-posedness and stability of evolution systems in A and various remarks and discussions are included for the reader's benefit; numerical simulations are included in Section 5 to illustrate the effectiveness of the proposed control design.

Notations. The symbols $\wedge$ and $\vee$ denote the infimum and supremum operators, respectively. These operators are also applied to more than two arguments. The symbol $'\text{col}'$ denotes the column operator.

The symbol $\times$ denotes the vector cross product operator.

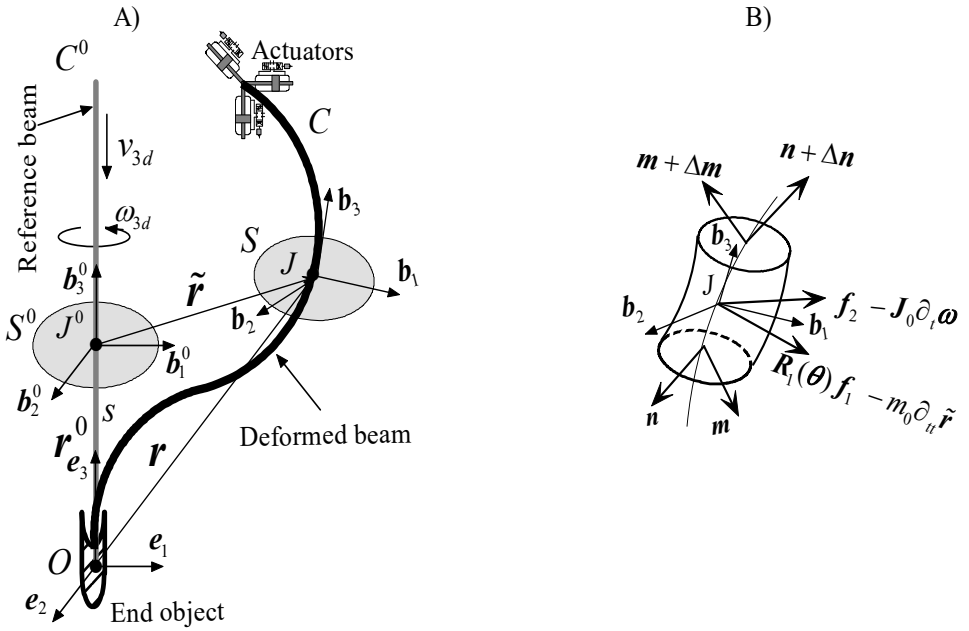

Figure 1.: A) Deformation geometry of the beam; B) Forces and moments acting on a beam element.

2. Mathematical model

A beam in space as shown in Fig. 1 is considered in this paper. The lower-end of the beam is connected to an end object, which can be a drill head for instance, via a fixed joint while the upper-end is connected to actuators that provide boundary control forces and moments. These actuators can be a XYZ-table fixed to a fixed structure (such as a off-shore platform), see AliExpress (2020) for example, equipped with tip motors. The XYZ-table is to provide boundary control forces while the tip motors are to provide boundary control moments. We assume that plane sections are rigid; and the beam material is (nonlinear) elastic, homogeneous and isotropic. In what follows, equations of motion are briefly derived, see Do (2017c) for details, for the purpose of the present paper.

2.1. *Kinematics*

The reference beam is represented by the reference configuration $\mathcal{B}^0$ of the beam in space describing by the position of the base straight line C^0 parameterized by its arclength coordinate s and the fixed basis $(\boldsymbol{b}_1^0, \boldsymbol{b}_2^0, \boldsymbol{b}_3^0)$, where $(\boldsymbol{b}_1^0, \boldsymbol{b}_2^0)$ are collinear with the principal axes of inertia of the cross section $S^0(s)$ through the base point J^0, see Figure 1A. The triple $(\boldsymbol{e}_1, \boldsymbol{e}_2, \boldsymbol{e}_3)$ is paralleled to $(\boldsymbol{b}_1^0, \boldsymbol{b}_2^0, \boldsymbol{b}_3^0)$. Thus, C^0 is described by the position vector $\boldsymbol{r}^0(s)$, which in the fixed basis is expressed as $\boldsymbol{r}^0(s) = 0\boldsymbol{e}_1 + 0\boldsymbol{e}_2 + s\boldsymbol{e}_3$. We denote by Γ the beam length in its reference state. The reference beam rotates around its base straight-line (axial axis) with a reference angular velocity ω_{3d} and axially moves with a reference linear velocity v_{3d}.

The actual configuration $\mathcal{B}$ of the curved beam is described by the actual position $C(s,t)$ of the base curve and the actual configuration $S(s,t)$ of cross sections through the base point J. The base curve is described by the position vector $\boldsymbol{r}(s,t)$ while the material cross section is described by the unit vectors $\{\boldsymbol{b}_1(s,t), \boldsymbol{b}_2(s,t), \boldsymbol{b}_3(s,t)\}$ with $\boldsymbol{b}_3$ being aligned with $\boldsymbol{r}_s(s,t)$ and $\boldsymbol{b}_3 = \boldsymbol{b}_1 \times \boldsymbol{b}_2$.

The deformation from $\mathcal{B}^0$ to $\mathcal{B}$ is achieved by means of the vector $\boldsymbol{r}(s,t)$ expressed in the local basis, i.e., $\boldsymbol{r}(s,t) = r_1(s,t)\boldsymbol{b}_1 + r_2(s,t)\boldsymbol{b}_2 + r_3(s,t)\boldsymbol{b}_3$, and the orthogonal tensor $\boldsymbol{R}_1(\boldsymbol{\theta}(s,t))$ describing the incremental rigid rotation suffered by $S^0(s)$ so that $\boldsymbol{b}_k(s,t) = \boldsymbol{R}_1(\boldsymbol{\theta}(s,t))\boldsymbol{b}_k^0(s), k = 1,2,3$ via the sequence $\theta_1 \to \theta_2 \to \theta_3$. The matrix $\boldsymbol{R}_1(\boldsymbol{\theta}(s,t))$ is given in components by:

$$\boldsymbol{R}_1(\boldsymbol{\theta}) = \begin{bmatrix} c_{\theta_2}c_{\theta_3} & -c_{\theta_2}s_{\theta_3} & s_{\theta_2} \\ c_{\theta_3}s_{\theta_1}s_{\theta_2} + c_{\theta_1}s_{\theta_3} & c_{\theta_1}c_{\theta_3} - s_{\theta_1}s_{\theta_2}s_{\theta_3} & -c_{\theta_2}s_{\theta_1} \\ s_{\theta_1}s_{\theta_3} - c_{\theta_1}c_{\theta_3}s_{\theta_2} & c_{\theta_3}s_{\theta_1} + c_{\theta_1}s_{\theta_2}s_{\theta_3} & c_{\theta_1}c_{\theta_2} \end{bmatrix}, \tag{1}$$

where $\boldsymbol{\theta} := \mathrm{col}(\theta_1, \theta_2, \theta_3)$; $c_{\theta_i} := \cos(\theta_i)$ and $s_{\theta_i} := \sin(\theta_i)$. This gives $\boldsymbol{b}_{ks} = \boldsymbol{R}_{1s}\boldsymbol{b}_k^0$, where $\boldsymbol{R}_{1s} = \boldsymbol{\mu} \times \boldsymbol{b}_k$ with $\boldsymbol{\mu}$ being the axial vector of $\boldsymbol{R}_{1s}\boldsymbol{R}_1^T$. The generalized strains (i.e., the stretch ε and the shear

strains η_1 and η_2) are expressed by the stretch vector $\boldsymbol{\nu} = \eta_1\boldsymbol{b}_1 + \eta_2\boldsymbol{b}_2 + (1+\varepsilon)\boldsymbol{b}_3$ in its local basis: $\boldsymbol{\nu} = \boldsymbol{r}_s$. Thus, we have

$$\begin{array}{l} \boldsymbol{r}_s = \eta_1\boldsymbol{b}_1 + \eta_2\boldsymbol{b}_2 + (1+\varepsilon)\boldsymbol{b}_3 \\ \boldsymbol{\mu} = \mu_1\boldsymbol{b}_1 + \mu_2\boldsymbol{b}_2 + \mu_3\boldsymbol{b}_3,\ \boldsymbol{\omega} = \omega_1\boldsymbol{b}_1 + \omega_2\boldsymbol{b}_2 + \omega_3\boldsymbol{b}_3, \\ \boldsymbol{b}_{ks} = \boldsymbol{\mu}\times\boldsymbol{b}_k,\ \boldsymbol{b}_{kt} = \boldsymbol{\omega}\times\boldsymbol{b}_k,\ (\boldsymbol{\mu}\times\boldsymbol{b}_k)_t = (\boldsymbol{\omega}\times\boldsymbol{b}_k)_s. \end{array} \tag{2}$$

From (1) and (2), we have

$$\begin{array}{l} \mathrm{col}(\eta_1,\eta_2,\varepsilon) = \boldsymbol{R}_1^T\boldsymbol{r}_s - \boldsymbol{r}_s^0, \\ \mathrm{col}(\mu_1,\mu_2,\mu_3) = \boldsymbol{R}_2^{-1}\mathrm{col}(\theta_{1s},\theta_{2s},\theta_{3s}),\ \boldsymbol{R}_2(\boldsymbol{\theta}) = \begin{bmatrix} \frac{c_{\theta_3}}{c_{\theta_2}} & -\frac{s_{\theta_3}}{c_{\theta_2}} & 0 \\ s_{\theta_3} & c_{\theta_3} & 0 \\ -c_{\theta_3}t_{\theta_2} & s_{\theta_3}t_{\theta_2} & 1 \end{bmatrix}, \\ \mathrm{col}(\omega_1,\omega_2,\omega_3) = \boldsymbol{R}_2^{-1}\mathrm{col}(\theta_{1t},\theta_{2t},\theta_{3t}), \end{array} \tag{3}$$

where $t_{\theta_2} := \tan(\theta_2)$.

2.2. *Kinetic*

Balancing linear and angular momentum on a beam element, see Figure1B, gives the equations of motion:

$$\begin{array}{l} m_0\tilde{\boldsymbol{r}}_{tt} = \boldsymbol{n}_s + \boldsymbol{R}_1(\boldsymbol{\theta})\boldsymbol{f}_1, \\ \boldsymbol{J}_0\boldsymbol{\omega}_t = \boldsymbol{m}_s + \boldsymbol{r}_s\times\boldsymbol{n} - \boldsymbol{\omega}\times\boldsymbol{J}_0\boldsymbol{\omega} + \boldsymbol{f}_2, \end{array} \tag{4}$$

where m_0 is the beam mass per unit length; $\boldsymbol{J}_0 = \mathrm{diag}(J_{01}, J_{02}, J_{03})$ is the mass moment matrix of inertia; $\boldsymbol{n}$ and $\boldsymbol{m}$ denote the contact force and moment vectors; and (see Fig. 1A)

$$\tilde{\boldsymbol{r}} = \boldsymbol{r} - \boldsymbol{r}^0. \tag{5}$$

The nonconservative force and moment vectors $\boldsymbol{f}_1$ and $\boldsymbol{f}_2$ are given in the body-fixed frame as

$$\begin{array}{l} \boldsymbol{f}_1 = -\boldsymbol{D}_{11}\boldsymbol{v} + \boldsymbol{f}_{10}(t), \\ \boldsymbol{f}_2 = -\boldsymbol{D}_{21}\boldsymbol{\omega} - \boldsymbol{D}_{22}(\boldsymbol{\omega}\otimes\boldsymbol{\omega})\boldsymbol{\omega} + \boldsymbol{f}_{20}(t), \end{array} \tag{6}$$

where $\boldsymbol{D}_{11}$, $\boldsymbol{D}_{21}$, and $\boldsymbol{D}_{22}$ are diagonal and positive definite matrices; $\boldsymbol{a}\otimes\boldsymbol{a} := \mathrm{diag}(a_1^2, a_2^2, a_3^2)$ with $\boldsymbol{a} = \mathrm{col}(a_1, a_2, a_3)$; and $\boldsymbol{f}_{10}(t)$ and $\boldsymbol{f}_{20}(t)$ are external disturbances bounded in L^2-norm (including the gravity), and $\boldsymbol{v} = v_1\boldsymbol{b}_1 + v_2\boldsymbol{b}_2 + v_3\boldsymbol{b}_3$ is the linear velocity vector with coordinates in the body-fixed frame, i.e.,

$$\boldsymbol{v} = \boldsymbol{R}_1^{-1}(\boldsymbol{\theta})\tilde{\boldsymbol{r}}_t. \tag{7}$$

Note that only linear damping is included in the translational dynamics while nonlinear damping is also included in the rotational dynamics, see (6), because in most applications the translational dynamics are much "slower" than the rotational dynamics. When $\theta_2 = \pm\frac{\pi}{2}$, there are singularities in (3). Thus, we use the unit quaternion vector $\boldsymbol{q} = \mathrm{col}(q_1, q_2, q_3, q_4)$ for attitude representation with $\|\boldsymbol{q}\|^2 = 1$ relating to $(\theta_1, \theta_2, \theta_3)$ via the sequence $\theta_1 \to \theta_2 \to \theta_3$ as follows, see Kuipers (2002):

$$\boldsymbol{q}(\boldsymbol{\theta}) = \begin{bmatrix} \cos(\frac{\theta_1}{2})\cos(\frac{\theta_2}{2})\cos(\frac{\theta_3}{2}) - \sin(\frac{\theta_1}{2})\sin(\frac{\theta_2}{2})\sin(\frac{\theta_3}{2}) \\ \sin(\frac{\theta_1}{2})\cos(\frac{\theta_2}{2})\cos(\frac{\theta_3}{2}) + \cos(\frac{\theta_1}{2})\sin(\frac{\theta_2}{2})\sin(\frac{\theta_3}{2}) \\ \cos(\frac{\theta_1}{2})\sin(\frac{\theta_2}{2})\cos(\frac{\theta_3}{2}) - \sin(\frac{\theta_1}{2})\cos(\frac{\theta_2}{2})\sin(\frac{\theta_3}{2}) \\ \cos(\frac{\theta_1}{2})\cos(\frac{\theta_2}{2})\sin(\frac{\theta_3}{2}) + \sin(\frac{\theta_1}{2})\sin(\frac{\theta_2}{2})\cos(\frac{\theta_3}{2}) \end{bmatrix}. \tag{8}$$

The rotational matrix $\boldsymbol{R}_1$ is given in terms of $\boldsymbol{q}$ as follows:

$$\boldsymbol{R}_1(\boldsymbol{q}) = \boldsymbol{I}_3 + 2q_1\boldsymbol{S}(\bar{\boldsymbol{q}}) + 2\boldsymbol{S}^2(\bar{\boldsymbol{q}}), \tag{9}$$

where $\bar{\boldsymbol{q}} := \mathrm{col}(q_2, q_3, q_4)$ and the matrix $\boldsymbol{S}(\boldsymbol{x})$ is defined as $\boldsymbol{S}(\boldsymbol{x})\boldsymbol{y} = \boldsymbol{x}\times\boldsymbol{y}$ for all $(\boldsymbol{x}, \boldsymbol{y}) \in \mathbb{R}^3$. Let us also define the matrix:

$$\boldsymbol{K}(\boldsymbol{q}) = \frac{1}{2}\begin{bmatrix} -\bar{\boldsymbol{q}}^T \\ q_1\boldsymbol{I}_3 + \boldsymbol{S}(\bar{\boldsymbol{q}}) \end{bmatrix}. \tag{10}$$

With (3), (7), (9), and (10), we can write (4) as the following system of PDEs:

$$\begin{array}{l} \tilde{\boldsymbol{r}}_t = \boldsymbol{R}_1(\boldsymbol{q})\boldsymbol{v}, \\ \boldsymbol{q}_t = \boldsymbol{K}(\boldsymbol{q})\boldsymbol{\omega}, \\ m_0\boldsymbol{v}_t = m_0(\boldsymbol{R}_1^{-1}(\boldsymbol{q}))_t\boldsymbol{R}_1(\boldsymbol{q})\boldsymbol{v} + \boldsymbol{R}_1^{-1}(\boldsymbol{q})\boldsymbol{n}_s + \boldsymbol{f}_1, \\ \boldsymbol{J}_0\boldsymbol{\omega}_t = \boldsymbol{m}_s - \boldsymbol{\omega}\times(\boldsymbol{J}_0\boldsymbol{\omega}) + \boldsymbol{r}_s\times\boldsymbol{n} + \boldsymbol{f}_2. \end{array} \tag{11}$$

The contact force and moment vectors $\boldsymbol{n}$ and $\boldsymbol{m}$ are given by:

$$\begin{array}{l} \boldsymbol{n}(s,t) = Q_1(s,t)\boldsymbol{b}_1 + Q_2(s,t)\boldsymbol{b}_2 + N(s,t)\boldsymbol{b}_3, \\ \boldsymbol{m}(s,t) = M_1(s,t)\boldsymbol{b}_1 + M_2(s,t)\boldsymbol{b}_2 + T(s,t)\boldsymbol{b}_3, \end{array} \tag{12}$$

where Q_1 and Q_2 are the shear forces; N is the axial force; M_1 and M_2 are the bending moments; and T is the twisting moment. Using the third-order Maclaurin series expansion of nonlinear stress-strain relations in Orthwein (1968) results in the constitutive equations:

$$\begin{aligned} &Q_i = G\bar{A}_i\eta_i,\ N = EA\varepsilon, \\ &M_i = EI_i\big(\mu_i - \tfrac{1}{2}\mu_i^2 + \tfrac{1}{3}\mu_i^3\big),\ T = GI_3\big(\mu_3 - \tfrac{1}{2}\mu_3^3 + \tfrac{1}{3}\mu_3^3\big), \end{aligned} \tag{13}$$

where $i = 1, 2$; E is the Young modulus; G is the shear modulus; $A, \bar{A}_1, \bar{A}_2$ are cross section and shear areas; $I_k, k = 1, 2, 3$ are principal mass moments of inertia about $\boldsymbol{b}_k$. It is noted that we use linear constitutive relations for Q_i and N while nonlinear ones for M_i and T to make them consistent with (6). The initial conditions are given by

$$\begin{aligned} &\tilde{\boldsymbol{r}}(s, t_0) = \tilde{\boldsymbol{r}}_{10}(s), \quad \tilde{\boldsymbol{r}}_t(s, t_0) = \tilde{\boldsymbol{r}}_{20}(s), \\ &\boldsymbol{\theta}(s, t_0) = \boldsymbol{\theta}_0(s), \quad \boldsymbol{\omega}(s, t_0) = \boldsymbol{\omega}_0(s). \end{aligned} \tag{14}$$

Finally, referring to Fig. 1A the boundary conditions are given by

$$\text{At } s = 0: \begin{cases} \theta_1 = \theta_2 = 0,\ \tilde{x} = \tilde{y} = 0, \\ m_P\ddot{\tilde{z}} = N + f_1^{B0}, \\ J_P\,\ddot{\theta}_3 = T + f_2^{B0}, \end{cases} \qquad \text{At } s = \Gamma: \begin{cases} \boldsymbol{M}_H\ddot{\tilde{\boldsymbol{r}}} = -\boldsymbol{n} + \boldsymbol{\phi}_{1B} + \boldsymbol{R}_1(\boldsymbol{q})\boldsymbol{f}_1^{B\Gamma}, \\ \dot{\boldsymbol{q}} = \boldsymbol{K}(\boldsymbol{q})\boldsymbol{\omega}, \\ \boldsymbol{J}_H\dot{\boldsymbol{\omega}} = -\boldsymbol{m} - \boldsymbol{\omega}\times(\boldsymbol{J}_H\boldsymbol{\omega}) + \boldsymbol{\phi}_{2B} + \boldsymbol{f}_2^{B\Gamma}, \end{cases} \tag{15}$$

where $(\tilde{x}, \tilde{y}, \tilde{z})$ are elements of $\tilde{\boldsymbol{r}}$ expressed in the fixed-coordinates, i.e., $\tilde{\boldsymbol{r}} = \tilde{x}\boldsymbol{e}_1 + \tilde{y}\boldsymbol{e}_e + \tilde{z}\boldsymbol{e}_3$, and

$$\text{At } s = 0: \begin{cases} f_1^{B0} = -d_{11}^0\dot{\tilde{z}} + f_{10}^{B0}, \\ f_2^{B0} = -d_{21}^0\dot{\theta}_3 - d_{22}^0\dot{\theta}_3^3 + f_{20}^{B0}, \end{cases} \quad \text{At } s = \Gamma: \begin{cases} \boldsymbol{f}_1^{B\Gamma} = -\boldsymbol{D}_{11}^\Gamma\boldsymbol{v} + \boldsymbol{f}_{10}^{B\Gamma}, \\ \boldsymbol{f}_2^{B\Gamma} = -\boldsymbol{D}_{21}^\Gamma\boldsymbol{\omega} - \boldsymbol{D}_{22}^\Gamma(\boldsymbol{\omega}\otimes\boldsymbol{\omega})\boldsymbol{\omega} + \boldsymbol{f}_{20}^{B\Gamma}, \end{cases} \tag{16}$$

and m_p and J_P are the mass and inertia moment of the end object; $\boldsymbol{M}_H$ and $\boldsymbol{J}_H$ are mass and inertia moment matrices of the actuator systems; d_{11}^0, d_{21}^0 and d_{22}^0 are positive damping constants; $\boldsymbol{D}_{ij}^\Gamma$ are positive definite and diagonal damping matrices; $\boldsymbol{\phi}_{1B}$ and $\boldsymbol{\phi}_{2B}$ are force and moment boundary control input vectors; and f_{i0}^0 and $\boldsymbol{f}_{i0}^\Gamma$ are external forces and moments on the end object and actuators.

To prepare for the control objective formulation and control design in the sequel, let $\boldsymbol{q}_d = \text{col}(q_{1d}, \bar{\boldsymbol{q}}_d)$ be the reference quaternion vector at $s = \Gamma$ defined by

$$\dot{\boldsymbol{q}}_d = \boldsymbol{K}(\boldsymbol{q}_d)\boldsymbol{\omega}_d, \tag{17}$$

with $\boldsymbol{q}_d(t_0) = \text{col}(1, 0, 0, 0)$ at the initial time t_0, i.e., zero reference attitude at the initial time. In (17), $\boldsymbol{\omega}_d = \text{col}(0, 0, \omega_{3d})$ and $\boldsymbol{K}(\boldsymbol{q}_d)$ is the value of $\boldsymbol{K}(\boldsymbol{q})$ evaluated at $\boldsymbol{q} = \boldsymbol{q}_d$. Define the attitude tracking errors as follows, see Do (2015):

$$\begin{aligned} &\xi_1 = q_{1d}q_1 + \bar{\boldsymbol{q}}_d^T\boldsymbol{q}, \\ &\bar{\boldsymbol{\xi}} = q_{1d}\bar{\boldsymbol{q}} - q_1\boldsymbol{S}(\bar{\boldsymbol{q}}_d)\bar{\boldsymbol{q}}, \end{aligned} \tag{18}$$

where the skew-symmetric matrix $\boldsymbol{S}(\boldsymbol{x})$ is defined as $\boldsymbol{S}(\boldsymbol{x})\boldsymbol{y} = \boldsymbol{x}\times\boldsymbol{y}$ for all $(\boldsymbol{x}, \boldsymbol{y}) \in \mathbb{R}^3$. Differentiating both sides of (18) along the solutions of (17) and the equation $\dot{\boldsymbol{q}} = \boldsymbol{K}(\boldsymbol{q})\boldsymbol{\omega}$ in (15) yields

$$\begin{aligned} &\dot{\xi}_1 = -\tfrac{1}{2}\bar{\boldsymbol{\xi}}^T(\boldsymbol{\omega} - \boldsymbol{\omega}_d), \\ &\dot{\bar{\boldsymbol{\xi}}} = \tfrac{1}{2}\boldsymbol{G}(\boldsymbol{\omega} - \boldsymbol{\omega}_d), \end{aligned} \tag{19}$$

where $\boldsymbol{G} = \xi_1\boldsymbol{I}_3 + \boldsymbol{S}(\bar{\boldsymbol{\xi}})$ with $\boldsymbol{I}_3$ being the 3×3 identity matrix.

Lemma 2.1: *Suppose that $\dot{\boldsymbol{\omega}}$ is governed by*

$$\dot{\boldsymbol{\omega}} = -(k+\epsilon)(\gamma\boldsymbol{G}^T\bar{\boldsymbol{\xi}} + \boldsymbol{\omega} - \boldsymbol{\omega}_d) - \gamma\dot{\boldsymbol{G}}^T\bar{\boldsymbol{\xi}} - \gamma\boldsymbol{G}^T\dot{\bar{\boldsymbol{\xi}}} + \dot{\boldsymbol{\omega}}_d, \tag{20}$$

where k, ϵ, and γ are positive constants, then $\bar{\boldsymbol{\xi}}(t)$ globally asymptotically tends to zero while $\xi_1(t)$ globally asymptotically tends to ± 1.

Proof. Consider the Lyapunov function candidate

$$U = 2k\gamma\|\bar{\boldsymbol{\xi}}\|^2 + \tfrac{1}{2}\|\gamma\boldsymbol{G}^T\bar{\boldsymbol{\xi}} + \boldsymbol{\omega} - \boldsymbol{\omega}_d\|^2, \tag{21}$$

whose derivative along the solutions of (20) and (19) is

$$\dot{U} = -k\gamma\|\boldsymbol{G}^T\bar{\boldsymbol{\xi}}\|^2 - k\|\boldsymbol{\omega} - \boldsymbol{\omega}_d\|^2 - \epsilon\|\gamma\boldsymbol{G}^T\bar{\boldsymbol{\xi}} + \boldsymbol{\omega} - \boldsymbol{\omega}_d\|^2, \tag{22}$$

which by Barbalat's lemma implies that $\lim_{t\to\infty}(\gamma\boldsymbol{G}^T(t)\bar{\boldsymbol{\xi}}(t) + \boldsymbol{\omega}(t) - \boldsymbol{\omega}_d(t)) = 0$, i.e., $\boldsymbol{\omega} - \boldsymbol{\omega}_d$ globally asymptotically tends to $-\gamma\boldsymbol{G}^T\bar{\boldsymbol{\xi}}$. Substituting this limit to (19) yields

$$\begin{aligned} &\dot{\xi}_1 = \tfrac{\gamma}{2}\bar{\boldsymbol{\xi}}^T\boldsymbol{G}^T\bar{\boldsymbol{\xi}}, \\ &\dot{\bar{\boldsymbol{\xi}}} = -\tfrac{\gamma}{2}\boldsymbol{G}\boldsymbol{G}^T\bar{\boldsymbol{\xi}}, \end{aligned} \tag{23}$$

Now, we consider the Lyapunov function candidates U_1 and $\bar{U}$, of which derivatives along the solutions of (23) as

$$\left\{\begin{array}{l} U_1 = \xi_1^2, \\ \bar{U} = \|\bar{\boldsymbol{\xi}}\|^2, \end{array}\right. \Rightarrow \left\{\begin{array}{l} \dot{U}_1 = \gamma\xi_1^2\|\bar{\boldsymbol{\xi}}\|^2, \\ \dot{\bar{U}} = -\gamma\xi_1^2\|\bar{\boldsymbol{\xi}}\|^2, \end{array}\right. \tag{24}$$

The ξ_1-subsystem is unstable. Instability of this subsystem implies that $\xi_1(t)$ asymptotically tends to a non-zero but bounded value if $\xi_1(t_0) \neq 0$. If $\xi_1(t_0) = 0$, arbitrarily small noise will drive $\xi_1(t_0)$ to a non-zero value $\xi_1(t)$ at some t since the ξ_1-subsystem is unstable. A non-zero $\xi_1(t)$ implies from the $\bar{\boldsymbol{\xi}}$-subsystem that $\bar{\boldsymbol{\xi}}(t)$ tends to zero asymptotically. Since $\xi_1^2(t) + \|\bar{\boldsymbol{\xi}}(t)\|^2 = 1$, $\xi_1(t)$ will eventually converge to 1 or -1. Asymptotic convergence of $\xi_1(t)$ to ± 1 and $\bar{\boldsymbol{\xi}}(t)$ to $\mathbf{0}$ implies that of $\boldsymbol{q} - \boldsymbol{q}_d$. This is because the identity quaternion $(1, \mathbf{0})$ represents a rotation of the negative identity quaternion $(-1, \mathbf{0})$ by 2π from the desired attitude, and is therefore the same physical orientation, see Do (2015).

3. Control objective

Before stating the control objective, we make the following assumption, which is reasonable in practice, on boundedness of initial values and external loads.

Assumption 3.1:

1) The initial values $\tilde{\boldsymbol{r}}_{10}(s), \tilde{\boldsymbol{r}}_{20}(s), \boldsymbol{\theta}_0(s), \boldsymbol{\omega}_0(s)$ are bounded in L^2-norm, i.e., there exists $\epsilon_0 \geq 0$ such that $\int_0^\Gamma (\|\tilde{\boldsymbol{r}}_{10}(s)\|^2 + \|\tilde{\boldsymbol{r}}_{20}(s)\|^2 + \|\boldsymbol{\theta}_0(s)\|^2 + \|\boldsymbol{\omega}_0(s)\|^2)ds \leq \epsilon_0$, where $\|\cdot\|$ denotes the Euclidean norm. Moreover, $\|\tilde{\boldsymbol{r}}_1(0,t_0)\|^2 + \|\tilde{\boldsymbol{r}}_2(0,t_0)\|^2 + \|\boldsymbol{\theta}(0,t_0)\|^2 + \|\boldsymbol{\omega}(0,t_0)\|^2$ and $\|\tilde{\boldsymbol{r}}(\Gamma,t_0)\|^2 + \|\tilde{\boldsymbol{r}}_t(\Gamma,t_0)\|^2 + \|\boldsymbol{\theta}(\Gamma,t_0)\|^2 + \|\boldsymbol{\omega}(\Gamma,t_0)\|^2$ are also bounded.

2) The external loads are bounded in appropriate norms, i.e. there exist nonnegative constants f_{i0}^M, f_{i0}^{B0M}, and $f_{i0}^{B\Gamma M}$ such that

$$\sup_{t\in[t_0,\infty)} \int_0^\Gamma \|\boldsymbol{f}_{i0}(s,t)\|^2 ds \leq f_{i0}^M,\ \sup_{t\in[t_0,\infty)} \|\boldsymbol{f}_{i0}^{B0}(t)\|^2 \leq f_{i0}^{B0M},\ \sup_{t\in[t_0,\infty)} \|\boldsymbol{f}_{i0}^{B\Gamma}(t)\|^2 \leq f_{i0}^{B\Gamma M}. \tag{25}$$

3) The reference velocities and accelerations $(v_{3d}, \dot{v}_{3d})$ and $(\omega_{3d}, \dot{\omega}_{3d})$ are bounded, i.e., there exist nonnegative constants $(v_{3d}^M, \bar{v}_{3d}^M)$ and $(\omega_{3d}, \bar{\omega}_{3d}^M)$ such that

$$\sup_{t\in[t_0,\infty)} |v_{3d}(t)| \leq v_{3d}^M,\ \sup_{t\in[t_0,\infty)} |\dot{v}_{3d}(t)| \leq \bar{v}_{3d}^M,\ \sup_{t\in[t_0,\infty)} |\omega_{3d}(t)| \leq \omega_{3d}^M,\ \sup_{t\in[t_0,\infty)} |\dot{\omega}_{3d}(t)| \leq \bar{\omega}_{3d}^M. \tag{26}$$

Control Objective 3.1: *Under Assumption 3.1, design the boundary control vectors $\boldsymbol{\phi}_{iB}, i = 1, 2$ such that the beam, of which the dynamics consist of (11)-(15), globally practically asymptotically track its reference beam in the sense that*

$$\mathcal{E}(t) \leq \mathcal{E}(t_0)e^{-c(t-t_0)} + c_0, \tag{27}$$

where c is a positive constant depending on the initial conditions, c_0 is a nonnegative constant, and $\mathcal{E}(t)$ is given by

$$\begin{aligned}
&\mathcal{E}(t) = \mathcal{E}^{0\Gamma}(t) + \mathcal{E}^{B0}(t) + \mathcal{E}^{B\Gamma}(t), \\
&\mathcal{E}^{0\Gamma}(t) = \int_0^\Gamma \big[\|\boldsymbol{v}(s,t) - \boldsymbol{v}_d(t)\|^2 + \|\boldsymbol{\omega}(s,t) - \boldsymbol{\omega}_d(t)\|^2 + \|\boldsymbol{\vartheta}(s,t)\|^2 + \|\boldsymbol{\mu}(s,t)\|^2 \\
&\qquad + (\mu_1^4(s,t) + \mu_2^4(s,t) + \mu_3^4(s,t))\big] ds, \\
&\mathcal{E}^{B0}(t) = (v_3(0,t) - v_{3d}(t))^2 + (\omega_3(0,t) - \omega_{3d}(t))^2, \\
&\mathcal{E}^{B\Gamma}(t) = \big\|\gamma_1(\tilde{\boldsymbol{r}}(\Gamma,t) - \tilde{\boldsymbol{r}}_d(t)) + \boldsymbol{R}_1(\boldsymbol{q}(\Gamma,t))(\boldsymbol{v}(\Gamma,t) - \boldsymbol{v}_d(t)) + \gamma\Gamma\boldsymbol{R}_1(\boldsymbol{q}(\Gamma,t))\boldsymbol{\vartheta}(\Gamma,t)\big\|^2 \\
&\qquad + \|\tilde{\boldsymbol{r}}(\Gamma,t) - \tilde{\boldsymbol{r}}_d(t)\|^2 + \|\gamma_2\boldsymbol{G}^T(\Gamma,t)\bar{\boldsymbol{\xi}}(\Gamma,t) + \boldsymbol{\omega}(\Gamma,t) - \boldsymbol{\omega}_d(t) + \gamma\Gamma\boldsymbol{\mu}(\Gamma,t)\|^2 + \|\bar{\boldsymbol{\xi}}(\Gamma,t)\|^2,
\end{aligned} \tag{28}$$

where γ, γ_1, and γ_2 are positive constants (to be chosen later), and

$$\begin{aligned}
&\dot{\tilde{\boldsymbol{r}}}_d = \boldsymbol{v}_d, \\
&\boldsymbol{v}_d = col(0, 0, v_{3d}), \\
&\boldsymbol{\vartheta} = col(\eta_1, \eta_2, \varepsilon).
\end{aligned} \tag{29}$$

Remark 3.1: *Since the constant c in (27) depends on the initial values, asymptotic tracking is achieved instead of exponential tracking. It can be seen that $\mathcal{E}(t)$ is a positive definite and radially unbounded functional of velocity errors, stretch, shear strain, bending and torsional curvatures. While*

this functional penalizes (translational and rotational) displacement and velocity errors of the actuated end, we only include translational and rotational velocity errors at the object end. This is because convergence of the translational and rotational displacements at any point of the beam including at the end object are ensured by convergence of $\mathcal{E}(t)$ via Sobolev embedding, see the last five inequalities in Lemma 3.1 below.

Remark 3.2: *It is clearly seen from (27) and (28) that when (27) is achieved (by the boundary control to be designed), the following desired features are obtained:*

- *The linear and angular velocity vectors $\boldsymbol{v}$ and $\boldsymbol{\omega}$ globally practically asymptotically track their reference linear and angular velocity vectors $\boldsymbol{v}_d$ and $\boldsymbol{\omega}_d$ in L^2-norm, see the term $\int_0^\Gamma \big[\|\boldsymbol{v}(s,t)-\boldsymbol{v}_d(t)\|^2+\|\boldsymbol{\omega}(s,t)-\boldsymbol{\omega}_d(t)\|^2\big]ds$ in the expression of $\mathcal{E}^{0\Gamma}$.*
- *The position and attitude, linear and angular velocities at the actuated end globally practically asymptotically track their reference values, see the expression of $\mathcal{E}^{B\Gamma}$ together with Lemma 2.1.*
- *The linear and angular velocity vectors at the unactuated end globally practically asymptotically track their reference values, see the expression of $\mathcal{E}^{B0}$.*
- *The stretch, shear strain, bending and torsional curvatures are globally practically asymptotically stabilized at the origin in L^2-norm, see the term $\int_0^\Gamma \big[\ \|\boldsymbol{\vartheta}(s,t)\|^2+\|\boldsymbol{\mu}(s,t)\|^2+(\mu_1^4(s,t)+\mu_2^4(s,t)+\mu_3^4(s,t))\big]ds$ in the expression of $\mathcal{E}^{0\Gamma}$.*

The above results together with Remark 3.1 ensure that the beam globally practically track its reference beam as we have defined that the reference beam is a straight-line moving axially with the linear reference velocity v_{3d} and rotating around it by the angular velocity ω_{3d}.

Several useful equalities and inequalities, which will be used in the control design and stability analysis, are given in the following lemma.

Lemma 3.1: *For all $t\geq t_0\geq 0$ and $s\in[0,\Gamma]$, the following equalities and inequalities hold:*

$$
\begin{aligned}
&1)\quad \boldsymbol{\omega}_s=\mu_{1t}\boldsymbol{b}_1+\mu_{2t}\boldsymbol{b}_2+\mu_{3t}\boldsymbol{b}_3,\\
&2)\quad \boldsymbol{\omega}^T(\boldsymbol{r}_s\times\boldsymbol{n})=\boldsymbol{n}^T(\eta_1\boldsymbol{b}_{1t}+\eta_2\boldsymbol{b}_{2t}+(1+\varepsilon)\boldsymbol{b}_{3t}),\\
&3)\quad \boldsymbol{\mu}^T(\boldsymbol{r}_s\times\boldsymbol{n})=-\boldsymbol{n}^T(\eta_1\boldsymbol{b}_{1s}+\eta_2\boldsymbol{b}_{2s}+(1+\varepsilon)\boldsymbol{b}_{3s}),\\
&4)\quad \boldsymbol{n}^T\tilde{\boldsymbol{r}}_{st}=Q_1\eta_{1t}+Q_2\eta_{2t}+N\varepsilon_t+\boldsymbol{\omega}^T(\boldsymbol{r}_s\times n),\\
&5)\quad \boldsymbol{n}^T(\boldsymbol{r}_s+\boldsymbol{r}_{ss}s)=Q_1\eta_1+Q_2\eta_2+N(1+\varepsilon)+Q_1\eta_{1s}s+Q_2\eta_{2s}s+N\varepsilon_s s+\boldsymbol{n}^T(\boldsymbol{\mu}\times\boldsymbol{r}_s)s,\\
&6)\quad \int_0^\Gamma\|\tilde{\boldsymbol{r}}(s,t)\|^2\leq 2\Gamma\|\tilde{\boldsymbol{r}}(\Gamma,t)\|^2+4\Gamma^2\int_0^\Gamma\|\tilde{\boldsymbol{r}}_s(s,t)\|^2ds,\\
&7)\quad \|\tilde{\boldsymbol{r}}(0,t)\|^2\leq 2\|\tilde{\boldsymbol{r}}(\Gamma,t)\|^2+4\Gamma\int_0^\Gamma\|\tilde{\boldsymbol{r}}_s(s,t)\|^2ds,\\
&8)\quad \int_0^\Gamma\|\tilde{\boldsymbol{r}}(s,t)\|^2ds\leq 2\int_0^\Gamma\|\boldsymbol{\vartheta}(s,t)\|^2ds+1152\Gamma^2\int_0^\Gamma\|\boldsymbol{\mu}(s,t)\|^2ds+96\Gamma(q_2^2(\Gamma,t)+q_3^2(\Gamma,t)),\\
&9)\quad \|col(q_1(0,t)-1,\bar{\boldsymbol{q}}(0,t))\|^2\leq 2\|col(q_1(\Gamma,t)-1,\bar{\boldsymbol{q}}(\Gamma,t))\|^2+\Gamma\int_0^\Gamma\|\boldsymbol{\mu}(s,t)\|^2ds,\\
&10)\quad \int_0^\Gamma\|col(q_1(s,t)-1,\bar{\boldsymbol{q}}(s,t))\|^2ds\leq 2\|col(q_1(\Gamma,t)-1,\bar{\boldsymbol{q}}(\Gamma,t))\|^2+\Gamma^2\int_0^\Gamma\|\boldsymbol{\mu}(s,t)\|^2ds,
\end{aligned}
\tag{30}
$$

where we have dropped the argument (s,t) for clarity. The inequality 8) is of its own interest because the right hand-side depends on $(q_2^2(\Gamma,t)+q_3^2(\Gamma,t))$ not on $q_1(\Gamma,t)$ and $q_4(\Gamma,t)$. This makes the boundary control design in this paper applicable to spinning beams such as drillers because the right hand-side of the inequality 8) does not depend on $\theta_3(\Gamma,t)$, which is inferred from (8), i.e., $q_2^2+q_3^2=\sin^2(\frac{\theta_1}{2})\cos^2(\frac{\theta_2}{2})+\cos^2(\frac{\theta_1}{2})\sin^2(\frac{\theta_2}{2})$ for all $s\in[0,\Gamma]$ and $t\in[t_0,\infty)$.

Proof. Proof of the first 5 equalities is given in the proof of Lemma 3.1 in Do (2017c) while the proof of the sixth and seventh inequalities is given in the proof of Lemma 2.1 in Do (2017e). We here provide the proof of the last three inequalities. From (5) and the first equation of (3), we have

$$\tilde{\boldsymbol{r}}_s=\boldsymbol{R}_1(\boldsymbol{q})\boldsymbol{\vartheta}+\boldsymbol{R}_1(\boldsymbol{q})\boldsymbol{e}_3-\boldsymbol{e}_3, \tag{31}$$

where $\boldsymbol{\vartheta}$ is defined in (29) and $\boldsymbol{e}_3:=\text{col}(0,0,1)$. By taking norm-2 both sides of (31) and applying Young's inequality together with the expression of $\boldsymbol{R}_1(\boldsymbol{q})$ in (9), we have

$$\|\tilde{\boldsymbol{r}}_s\|^2\leq 2\|\boldsymbol{\vartheta}\|^2+48(q_2^2+q_3^2). \tag{32}$$

Using the simplified Poincaré inequality, see proof of Lemma 2.1 in Do (2017e) and integrating both sides of (32) from 0 to Γ give

$$
\begin{aligned}
\int_0^\Gamma\|\tilde{\boldsymbol{r}}_s\|^2ds&\leq 2\int_0^\Gamma\|\boldsymbol{\vartheta}\|^2ds+48\int_0^\Gamma(q_2^2+q_3^2)ds\\
&\leq 2\int_0^\Gamma\|\boldsymbol{\vartheta}\|^2ds+192\int_0^\Gamma(q_{2s}^2+q_{3s}^2)ds+96\Gamma(q_2^2(\Gamma,t)+q_3^2(\Gamma,t))\\
&\leq 2\int_0^\Gamma\|\boldsymbol{\vartheta}\|^2ds+1152\Gamma^2\int_0^\Gamma\|\boldsymbol{\mu}\|^2ds+96\Gamma(q_2^2(\Gamma,t)+q_3^2(\Gamma,t)),
\end{aligned}
\tag{33}
$$

where we have use $\boldsymbol{q}_s = \boldsymbol{K}(\boldsymbol{q})\boldsymbol{\mu} \Rightarrow \|\boldsymbol{q}_s\|^2 \leq 6\|\boldsymbol{\mu}\|^2$ with $\boldsymbol{K}(\boldsymbol{q})$ given in (10), which completes proof of the inequality 8). Proof of the inequality 9) is similar to that of the inequality 7) with the use of $|q_1 - 1\ \bar{\boldsymbol{q}}^T|_s^T = \boldsymbol{q}_s = \boldsymbol{K}(\boldsymbol{q})\boldsymbol{\mu}$ and $\boldsymbol{K}^T(\boldsymbol{q})\boldsymbol{K}(\boldsymbol{q}) = \frac{1}{4}$. The inequality 10) can be proved by applying the simplified Poincaré inequality to $\| \, |q_1 - 1\ \bar{\boldsymbol{q}}^T|^T\|^2$. □

4. Control design

4.1. *Abstract formulation*

The abstract formulation in Do (2016) is applied here to represent the beam dynamics as an evolution system for control design and stability analysis. Let $L^2(\mathcal{D})$ denote the L^2-space with the norm $\|.\|_{L^2}$ and inner product $\langle .,. \rangle_{L^2}$ and $W^{m,n}(\mathcal{D})$, with (m,n) being integers, denote the Sobolev space of order m and degree n, see Adams and Fournier (2003), and $\mathcal{D} := [0, \Gamma]$. Considering $s \in \mathcal{D}$ as the parameter defined at every $t \geq t_0$, we can regard $\tilde{\boldsymbol{r}}(s,t)$, $\boldsymbol{q}(s,t)$, $\boldsymbol{v}(s,t)$, and $\boldsymbol{\omega}(s,t)$ as $\tilde{\boldsymbol{r}}(t) \in (W^{2,2}(\mathcal{D}))^3$, $\boldsymbol{q}(t) \in (W^{2,2}(\mathcal{D}))^4$, $\boldsymbol{v}(t) \in (L^2(\mathcal{D}))^3$, $\boldsymbol{\omega}(t) \in (L^2(\mathcal{D}))^3$, respectively. Similarly, $\tilde{z}(0,t)$, $\dot{\tilde{z}}(0,t)$, $\theta_3(0,t)$, and $\dot{\theta}_3(0,t)$ are regarded as $\tilde{z}^{B0}(t) \in \mathbb{R}$, $v_3^{B0}(t) \in \mathbb{R}$, $\theta_3^{B0}(t) \in \mathbb{R}$, $\omega_3^{B0}(t) \in \mathbb{R}$, respectively, and the similar notations are used for $x(0,t)$ and $y(0,t)$. Moreover, $\tilde{\boldsymbol{r}}(\Gamma,t)$, $\dot{\tilde{\boldsymbol{r}}}(\Gamma,t)$, $\boldsymbol{q}(\Gamma,t)$, and $\boldsymbol{\omega}(\Gamma,t)$ are considered as $\tilde{\boldsymbol{r}}_1^{B\Gamma}(t) \in \mathbb{R}^3$, $\tilde{\boldsymbol{r}}_2^{B\Gamma}(t) \in \mathbb{R}^3$, $\boldsymbol{q}^{B\Gamma}(t) \in \mathbb{R}^4$, $\boldsymbol{\omega}^{B\Gamma}(t) \in \mathbb{R}^3$, respectively. Let us also define $\mathbb{D}\phi(s) := \frac{\partial \phi}{\partial s}$. Thus, we can write the beam system (11) in the following evolution system (abstract form):

$$\begin{aligned}
&\tfrac{d\tilde{\boldsymbol{r}}}{dt} = \boldsymbol{R}_1(\boldsymbol{q})\boldsymbol{v},\ \tfrac{d\boldsymbol{q}}{dt} = \boldsymbol{K}(\boldsymbol{q})\boldsymbol{\omega},\\
&m_0 \tfrac{d\boldsymbol{v}}{dt} = m_0(\boldsymbol{R}_1^{-1}(\boldsymbol{q}))_t \boldsymbol{R}_1(\boldsymbol{q})\boldsymbol{v} + \boldsymbol{R}_1^{-1}(\boldsymbol{q})\mathbb{D}\boldsymbol{n} + \boldsymbol{f}_1,\\
&\boldsymbol{J}_0 \tfrac{d\boldsymbol{\omega}}{dt} = \mathbb{D}\boldsymbol{m} - \boldsymbol{\omega} \times (\boldsymbol{J}_0\boldsymbol{\omega}) + \mathbb{D}\boldsymbol{r} \times \boldsymbol{n} + \boldsymbol{f}_2.
\end{aligned} \tag{34}$$

The boundary conditions (15) are written as:

$$\begin{array}{ll}
\text{At } s = 0: & \text{At } s = \Gamma:\\
\begin{cases}
\theta_1^{B0} = \theta_2^{B0} = 0, \tilde{x}^{B0} = \tilde{y}^{B0} = 0,\\
\tfrac{d\tilde{z}^{B0}}{dt} = v_3^{B0},\ \tfrac{d\theta_3^{B0}}{dt} = \omega_3^{B0},\\
m_P \tfrac{dv_3^{B0}}{dt} = N^{B0} + f_1^{B0},\\
J_P \tfrac{d\omega_3^{B0}}{dt} = T^{B0} + f_2^{B0},
\end{cases} &
\begin{cases}
\tfrac{d\tilde{\boldsymbol{r}}_1^{B\Gamma}}{dt} = \tilde{\boldsymbol{r}}_2^{B\Gamma},\\
\tfrac{d\boldsymbol{q}^{B\Gamma}}{dt} = \boldsymbol{K}(\boldsymbol{q}^{B\Gamma})\boldsymbol{\omega}^{B\Gamma},\\
\boldsymbol{M}_H \tfrac{d\tilde{\boldsymbol{r}}_2^{B\Gamma}}{dt} = -\boldsymbol{n}^{B\Gamma} + \boldsymbol{\phi}_{1B} + \boldsymbol{f}_1^{B\Gamma},\\
\boldsymbol{J}_H \tfrac{d\boldsymbol{\omega}^{B\Gamma}}{dt} = -\boldsymbol{m}^{B\Gamma} - \boldsymbol{\omega}^{B\Gamma} \times (\boldsymbol{J}_H\boldsymbol{\omega}^{B\Gamma}) + \boldsymbol{\phi}_{2B} + \boldsymbol{f}_2^{B\Gamma},
\end{cases}
\end{array} \tag{35}$$

where $N^{B0}(t)$ and $T^{B0}(t)$ are the values of $N(t)$ and $T(t)$ evaluated at $s = 0$; and $\boldsymbol{n}^{B\Gamma}(t)$ and $\boldsymbol{m}^{B\Gamma}(t)$ are the values of $\boldsymbol{n}(t)$ and $\boldsymbol{m}(t)$ evaluated at $s = \Gamma$.

4.2. *Control design*

To design the boundary control vectors $\boldsymbol{\phi}_{iB}, i = 1, 2$, we consider the following Lyapunov functional candidate:

$$U = U_0 + U_1 + U_B \tag{36}$$

where the functionals U_0, U_1, and U_2 are chosen as follows:

$$\begin{aligned}
U_0 &= \tfrac{m_0}{2}\|\boldsymbol{v} - \boldsymbol{v}_d\|_{L^2}^2 + \tfrac{1}{2}\langle \boldsymbol{\omega} - \boldsymbol{\omega}_d, \boldsymbol{J}_0(\boldsymbol{\omega} - \boldsymbol{\omega}_d)\rangle_{L^2} + \tfrac{1}{2}\textstyle\sum_{i=1}^2 G\bar{A}_i\|\eta_i\|_{L^2}^2 + \tfrac{1}{2}EA\|\varepsilon\|_{L^2}^2\\
&\quad + \textstyle\sum_{i=1}^2 EI_i\langle \mu_i, (\tfrac{1}{2}\mu_i - \tfrac{1}{6}\mu_i^2 + \tfrac{1}{12}\mu_i^3)\rangle_{L^2} + GI_3\langle \mu_3, (\tfrac{1}{2}\mu_3 - \tfrac{1}{6}\mu_3^2 + \tfrac{1}{12}\mu_3^3)\rangle_{L^2},\\
U_1 &= \gamma m_0\langle \mathbb{D}\boldsymbol{r} - \varrho\boldsymbol{R}_1(\boldsymbol{q})\mathbb{D}\boldsymbol{r}^0, \boldsymbol{R}_1(\boldsymbol{q})(\boldsymbol{v} - \boldsymbol{v}_d)s\rangle_{L^2} + \gamma\langle \boldsymbol{\mu}, \boldsymbol{J}_0(\boldsymbol{\omega} - \boldsymbol{\omega}_d)s\rangle_{L^2},\\
U_B &= \tfrac{m_P}{2}(v_3^{B0} - v_{3d})^2 + \tfrac{J_P}{2}(\omega_3^{B0} - \omega_{3d})^2 + \tfrac{1}{2}\big(\gamma_1(\tilde{\boldsymbol{r}}_1^{B\Gamma} - \tilde{\boldsymbol{r}}_d) + \boldsymbol{R}_1(\boldsymbol{q}^{B\Gamma})(\boldsymbol{v}^{B\Gamma} - \boldsymbol{v}_d) + \gamma\Gamma\boldsymbol{R}_1(\boldsymbol{q}^{B\Gamma})\boldsymbol{\vartheta}^{B\Gamma}\big)^T\\
&\quad \times \boldsymbol{M}_H\big(\gamma_1(\tilde{\boldsymbol{r}}_1^{B\Gamma} - \tilde{\boldsymbol{r}}_d) + \boldsymbol{R}_1(\boldsymbol{q}^{B\Gamma})(\boldsymbol{v}^{B\Gamma} - \boldsymbol{v}_d) + \gamma\Gamma\boldsymbol{R}_1(\boldsymbol{q}^{B\Gamma})\boldsymbol{\vartheta}^{B\Gamma}\big) + \gamma_1 k_{1B}\|\tilde{\boldsymbol{r}}_1^{B\Gamma} - \tilde{\boldsymbol{r}}_d\|^2\\
&\quad + \tfrac{1}{2}\big(\gamma_2\boldsymbol{G}^T\bar{\boldsymbol{\xi}} + \boldsymbol{\omega}^{B\Gamma} - \boldsymbol{\omega}_d + \gamma\Gamma\boldsymbol{\mu}^{B\Gamma}\big)^T\boldsymbol{J}_H\big(\gamma_2\boldsymbol{G}^T\bar{\boldsymbol{\xi}} + \boldsymbol{\omega}^{B\Gamma} - \boldsymbol{\omega}_d + \gamma\Gamma\boldsymbol{\mu}^{B\Gamma}\big) + 2\gamma_2 k_{2B}\|\bar{\boldsymbol{\xi}}\|^2,
\end{aligned} \tag{37}$$

where γ, γ_1, γ_2, k_{1B},and k_{2B} are positive constants to be chosen later. The constant $0 \leq \varrho \leq 1$ (to be specified later) plays the role of handling both large and small bending stiffness relatively to the shear stiffness. We elaborate the choice of the Lyapunov function candidate U in (36) with U_0, U_1, and U_2 being given in (37) in the following remark.

Remark 4.1: *The function U_0 is the sum of kinetic and potential energies of the beam with respect*

to its reference. The choice of U_1 is motivated by the backstepping method Krstic, Kanellakopoulos, and Kokotovic (1995), for example with the first equation of (3) and (29) it can be shown that $\frac{d\tilde{\boldsymbol{r}}_1}{dt} = \gamma m_0 \boldsymbol{\vartheta} s$ (with a note that $\mathbb{D}\boldsymbol{r} = \boldsymbol{R}_1(\boldsymbol{q})\boldsymbol{\vartheta} + \boldsymbol{R}_1(\boldsymbol{q})\mathbb{D}\boldsymbol{r}^0$, see (3)) is globally exponentially stable at the origin by an appropriate boundary control. The function U_B puts appropriate weights on translational displacements and velocities of the beam at the boundaries with respect to its reference, see also Remark 3.1.

We now find the bounds of U. Using $\frac{1}{3}x^2 + \frac{1}{12}x^4 \leq \frac{1}{2}(x^2 - \frac{1}{3}x^3 + \frac{1}{4}x^4) \leq \frac{2}{3}x^2 + \frac{1}{6}x^4$ for all $x \in \mathbb{R}$, we can bound U_0 as:

$$\begin{aligned}
U_0 \geq\ & \tfrac{m_0}{2}\|\boldsymbol{v} - \boldsymbol{v}_d\|_{L^2}^2 + \tfrac{\lambda_m(\boldsymbol{J}_0)}{2}\|\boldsymbol{\omega} - \boldsymbol{\omega}_d\|_{L^2}^2 + \tfrac{1}{2}(G\bar{A}_1 \wedge G\bar{A}_2 \wedge EA)\|\boldsymbol{\vartheta}\|_{L^2}^2 + \tfrac{1}{3}(EI_1 \wedge EI_2 \wedge GI_3)\|\boldsymbol{\mu}\|_{L^2}^2 \\
& + \tfrac{1}{12}(EI_1 \wedge EI_2 \wedge GI_3)\big\langle 1, \mu_1^4 + \mu_2^4 + \mu_3^4\big\rangle_{L^2}, \\
U_0 \leq\ & \tfrac{m_0}{2}\|\boldsymbol{v} - \boldsymbol{v}_d\|_{L^2}^2 + \tfrac{\lambda_M(\boldsymbol{J}_0)}{2}\|\boldsymbol{\omega} - \boldsymbol{\omega}_d\|_{L^2}^2 + \tfrac{1}{2}(G\bar{A}_1 \vee G\bar{A}_2 \vee EA)\|\boldsymbol{\vartheta}\|_{L^2}^2 + \tfrac{2}{3}(EI_1 \vee EI_2 \vee GI_3)\|\boldsymbol{\mu}\|_{L^2}^2 \\
& + \tfrac{1}{6}(EI_1 \vee EI_2 \vee GI_3)\big\langle 1, \mu_1^4 + \mu_2^4 + \mu_3^4\big\rangle_{L^2},
\end{aligned} \tag{38}$$

where $\lambda_m(\bullet)$ and $\lambda_M(\bullet)$ denote the minimum and maximum eigenvalues of $\bullet$, respectively. Since $\mathbb{D}\boldsymbol{r} = \boldsymbol{R}_1(\boldsymbol{q})\boldsymbol{\vartheta} + \boldsymbol{R}_1(\boldsymbol{q})\mathbb{D}\boldsymbol{r}^0$, (7), an application of Young's inequality results in the bound of $|U_1|$ as follows

$$\begin{aligned}
|U_1| \leq\ & \gamma\Gamma m_0(\varrho_{01} + (1-\varrho)\varrho_{03})\|\boldsymbol{v} - \boldsymbol{v}_d\|_{L^2}^2 + \gamma\Gamma\lambda_M(\boldsymbol{J}_0)\varrho_{02}\|\boldsymbol{\omega} - \boldsymbol{\omega}_d\|_{L^2}^2 \\
& + \tfrac{\gamma\Gamma m_0}{4\varrho_{01}}\|\boldsymbol{\vartheta}\|_{L^2}^2 + \tfrac{\gamma\Gamma\lambda_M(\boldsymbol{J}_0)}{4\varrho_{02}}\|\boldsymbol{\mu}\|_{L^2}^2 + \tfrac{\gamma\Gamma^2 m_0(1-\varrho)}{4\varrho_{03}},
\end{aligned} \tag{39}$$

where $\varrho_{0i}, i = 1, 2, 3$ are positive constants to be determined. We can calculate the bounds of U_2 as follows

$$\begin{aligned}
U_B \geq\ & \tfrac{m_P}{2}(v_3^{B0} - v_{3d})^2 + \tfrac{J_P}{2}(\omega_3^{B0} - \omega_{3d})^2 + \tfrac{\lambda_m(\boldsymbol{M}_H)}{2}\|\gamma_1(\tilde{\boldsymbol{r}}_1^{B\Gamma} - \tilde{\boldsymbol{r}}_d) + \boldsymbol{R}_1(\boldsymbol{q}^{B\Gamma})(\boldsymbol{v}^{B\Gamma} - \boldsymbol{v}_d) + \gamma\Gamma\boldsymbol{R}_1(\boldsymbol{q}^{B\Gamma})\boldsymbol{\vartheta}^{B\Gamma}\|^2 \\
& + \gamma_1 k_{1B}\|\tilde{\boldsymbol{r}}_1^{B\Gamma} - \tilde{\boldsymbol{r}}_d\|^2 + \tfrac{\lambda_m(\boldsymbol{J}_H)}{2}\|\gamma_2\boldsymbol{G}^T\bar{\boldsymbol{\xi}} + \boldsymbol{\omega}^{B\Gamma} - \boldsymbol{\omega}_d + \gamma\Gamma\boldsymbol{\mu}^{B\Gamma}\|^2 + 2\gamma_2 k_{2B}\|\bar{\boldsymbol{\xi}}\|^2, \\
U_B \leq\ & \tfrac{m_P}{2}(v_3^{B0} - v_{3d})^2 + \tfrac{J_P}{2}(\omega_3^{B0} - \omega_{3d})^2 + \tfrac{\lambda_M(\boldsymbol{M}_H)}{2}\|\gamma_1(\tilde{\boldsymbol{r}}_1^{B\Gamma} - \tilde{\boldsymbol{r}}_d) + \boldsymbol{R}_1(\boldsymbol{q}^{B\Gamma})(\boldsymbol{v}^{B\Gamma} - \boldsymbol{v}_d) + \gamma\Gamma\boldsymbol{R}_1(\boldsymbol{q}^{B\Gamma})\boldsymbol{\vartheta}^{B\Gamma}\|^2 \\
& + \gamma_1 k_{1B}\|\tilde{\boldsymbol{r}}_1^{B\Gamma} - \tilde{\boldsymbol{r}}_d\|^2 + \tfrac{\lambda_M(\boldsymbol{J}_H)}{2}\|\gamma_2\boldsymbol{G}^T\bar{\boldsymbol{\xi}} + \boldsymbol{\omega}^{B\Gamma} - \boldsymbol{\omega}_d + \gamma\Gamma\boldsymbol{\mu}^{B\Gamma}\|^2 + 2\gamma_2 k_{2B}\|\bar{\boldsymbol{\xi}}\|^2,
\end{aligned} \tag{40}$$

Using (38), (39), (40), and $U_0 - |U_1| + U_B \leq U \leq U_0 + |U_1| + U_B$, we can bound U as follows:

$$-\varrho_0 + c_1\,\mathcal{E} \leq U \leq c_2\mathcal{E} + \varrho_0, \tag{41}$$

where $\mathcal{E}$ is defined in (28), and the constants c_1, c_2, and ϱ_0 are given by

$$\begin{aligned}
c_1 =\ & \big[\tfrac{m_0}{2} - \gamma\Gamma m_0(\varrho_{01} + (1-\varrho)\varrho_{03})\big] \wedge \big[\tfrac{\lambda_m(\boldsymbol{J}_0)}{2} - \gamma\Gamma\varrho_{02}\lambda_M(\boldsymbol{J}_0)\big] \wedge \big[\tfrac{1}{2}(EA \wedge G\bar{A}_1 \wedge G\bar{A}_2) - \tfrac{\gamma\Gamma m_0}{4\varrho_{01}}\big] \\
& \wedge \big[\tfrac{1}{3}(EI_1 \wedge EI_2 \wedge GI_3) - \tfrac{\gamma\Gamma\lambda_M(\boldsymbol{J}_0)}{4\varrho_{02}}\big] \wedge \tfrac{1}{12}(EI_1 \wedge EI_2 \wedge GI_3) \wedge \big[\tfrac{\lambda_m(\boldsymbol{M}_{2H})}{2}\big] \wedge \tfrac{m_P}{2} \wedge \tfrac{J_P}{2} \wedge \tfrac{\lambda_m(\boldsymbol{M}_H)}{2} \\
& \wedge \tfrac{\lambda_m(\boldsymbol{J}_H)}{2} \wedge k_{1B}\gamma_1 \wedge 2\gamma_2 k_{2B}, \\
c_2 =\ & \big[\tfrac{m_0}{2} + \gamma\Gamma m_0(\varrho_{01} + (1-\varrho)\varrho_{03})\big] \vee \big[\tfrac{\lambda_M(\boldsymbol{J}_0)}{2} + \gamma\Gamma\varrho_{02}\lambda_M(\boldsymbol{J}_0)\big] \vee \big[\tfrac{1}{2}(EA \vee G\bar{A}_1 \vee G\bar{A}_2) + \tfrac{\gamma\Gamma m_0}{4\varrho_{01}}\big] \\
& \vee \big[\tfrac{2}{3}(EI_1 \vee EI_2 \vee GI_3) + \tfrac{\gamma\Gamma\lambda_M(\boldsymbol{J}_0)}{4\varrho_{02}}\big] \vee \tfrac{1}{6}(EI_1 \vee EI_2 \vee GI_3) \vee \big[\tfrac{\lambda_M(\boldsymbol{M}_{2H})}{2}\big] \vee \tfrac{m_P}{2} \vee \tfrac{J_P}{2} \vee \tfrac{\lambda_M(\boldsymbol{M}_H)}{2} \\
& \vee \tfrac{\lambda_M(\boldsymbol{J}_H)}{2} \vee \gamma_1 k_{1B} \vee 2\gamma_2 k_{2B}, \\
\varrho_0 =\ & \tfrac{\gamma\Gamma^2 m_0(1-\varrho)}{4\varrho_{03}}.
\end{aligned} \tag{42}$$

The constants γ, $\varrho_{0i}, i = 1, 2, 3$, and ϱ are chosen such that

$$c_1 \geq c_1^\diamond, \tag{43}$$

where $c_1^\diamond$ is a strictly positive constant. This is always possible by choosing a small γ for given $\varrho_{0i}, i = 1, 2, 3$, and ϱ. Thus, U is a proper functional of $\mathcal{E}$.

We now calculate the infinitesimal generator $\mathcal{L}U$. It is obvious from (36) that

$$\mathcal{L}U = \mathcal{L}U_0 + \mathcal{L}U_1 + \mathcal{L}U_B, \tag{44}$$

where $\mathcal{L}U_0$, $\mathcal{L}U_1$, and $\mathcal{L}U_B$ are detailed in what follows.

Calculation of $\mathcal{L}U_0$: Differentiating U_0 given in (37) along the solutions of (34) yields:

$$\begin{aligned}
\mathcal{L}U_0 =\ & \big\langle \boldsymbol{v} - \boldsymbol{v}_d, m_0(\boldsymbol{R}_1^{-1}(\boldsymbol{q}))_t\boldsymbol{R}_1(\boldsymbol{q})\boldsymbol{v} + \boldsymbol{R}_1^{-1}(\boldsymbol{q})\mathbb{D}\boldsymbol{n} + \boldsymbol{f}_1 - m_0\dot{\boldsymbol{v}}_d\big\rangle_{L^2} \\
& + \big\langle \boldsymbol{\omega} - \boldsymbol{\omega}_d, \mathbb{D}\boldsymbol{m} - \boldsymbol{\omega} \times (\boldsymbol{J}_0\boldsymbol{\omega}) + \mathbb{D}\boldsymbol{r} \times \boldsymbol{n} + \boldsymbol{f}_2 - \boldsymbol{J}_0\dot{\boldsymbol{\omega}}_d\big\rangle_{L^2} \\
& + \textstyle\sum_{i=1}^2 G\bar{A}_i\big\langle \eta_{it}, \eta_i\big\rangle_{L^2} + EA\big\langle \varepsilon_t, \varepsilon\big\rangle_{L^2} + \sum_{i=1}^2 EI_i\big\langle \mu_{it}, \big(\mu_i - \tfrac{1}{2}\mu_i^2 + \tfrac{1}{3}\mu_i^3\big)\big\rangle_{L^2} \\
& + GI_3\big\langle \mu_{3t}, \big(\mu_3 - \tfrac{1}{2}\mu_3^2 + \tfrac{1}{3}\mu_3^3\big)\big\rangle_{L^2}.
\end{aligned} \tag{45}$$

Before calculating the upper-bound of $\mathcal{L}U_0$, we note that

$$\begin{aligned}
&\big\langle \boldsymbol{v}, (\boldsymbol{R}_1^{-1}(\boldsymbol{q}))_t \boldsymbol{R}_1(\boldsymbol{q})\boldsymbol{v}\big\rangle_{L^2} = 0,\\
&\big\langle \boldsymbol{\omega}, \boldsymbol{\omega}\times(\boldsymbol{J}_0\boldsymbol{\omega})\big\rangle_{L^2} = 0,\\
&\big\langle \boldsymbol{v}, \boldsymbol{R}_1^{-1}(\boldsymbol{q})\mathbb{D}\boldsymbol{n}\big\rangle_{L^2} = \big\langle \tilde{\boldsymbol{r}}_t, \mathbb{D}\boldsymbol{n}\big\rangle_{L^2}\\
&\qquad\qquad = (\boldsymbol{n}^{B\Gamma})^T\tilde{\boldsymbol{r}}^{B\Gamma} - (\boldsymbol{n}^{B0})^T\tilde{\boldsymbol{r}}^{B0} - \big\langle \boldsymbol{n}, \mathbb{D}\tilde{\boldsymbol{r}}_t\big\rangle_{L^2}\\
&\qquad\qquad = (\boldsymbol{n}^{B\Gamma})^T\tilde{\boldsymbol{r}}^{B\Gamma} - (\boldsymbol{n}^{B0})^T\tilde{\boldsymbol{r}}^{B0} - \big\langle \boldsymbol{\omega}, \mathbb{D}\boldsymbol{r}\times\boldsymbol{n}\big\rangle_{L^2} - \textstyle\sum_{i=1}^2 G\bar{A}_i\big\langle \eta_{it}, \eta_i\big\rangle_{L^2} - EA\big\langle \varepsilon_t, \varepsilon\big\rangle_{L^2},\\
&\big\langle \boldsymbol{\omega}, \mathbb{D}\boldsymbol{m}\big\rangle_{L^2} = (\boldsymbol{m}^{B\Gamma})^T\boldsymbol{\omega}^{B\Gamma} - (\boldsymbol{m}^{B0})^T\boldsymbol{\omega}^{B0} - \big\langle \boldsymbol{m}, \mathbb{D}\boldsymbol{\omega}\big\rangle_{L^2}\\
&\quad = (\boldsymbol{m}^{B\Gamma})^T\boldsymbol{\omega}^{B\Gamma} - (\boldsymbol{m}^{B0})^T\boldsymbol{\omega}^{B0} - \textstyle\sum_{i=1}^2 EI_i\big\langle \mu_{it}, \mu_i - \frac{1}{2}\mu_i^2 + \frac{1}{3}\mu_i^3\big)\big\rangle_{L^2} + GI_3\big\langle \mu_{3t}, \big(\mu_3 - \frac{1}{2}\mu_3^2 + \frac{1}{3}\mu_3^3\big)\big\rangle_{L^2},
\end{aligned} \tag{46}$$

where Inequalities 1) and 4) in Lemma 3.1, see (30), and integration by parts have been used to obtain the last two equations. Using (46), integration by parts, and Young's inequality, we can find the upper-bound of $\mathcal{L}U_0$ as follows

$$\begin{aligned}
\mathcal{L}U_0 \le\ & \big[(\boldsymbol{n}^{B\Gamma})^T\boldsymbol{R}_1(\boldsymbol{q}^{B\Gamma})(\boldsymbol{v}^{B\Gamma} - \boldsymbol{v}_d) - (\boldsymbol{n}^{B0})^T\boldsymbol{R}_1(\boldsymbol{q}^{B0})(\boldsymbol{v}^{B0} - \boldsymbol{v}_d)\big]\\
&+\big[(\boldsymbol{m}^{B\Gamma})^T(\boldsymbol{\omega}^{B\Gamma} - \boldsymbol{\omega}_d) - (\boldsymbol{m}^{B0})^T(\boldsymbol{\omega}^{B0} - \boldsymbol{\omega}_d)\big]\\
&+m_0(\epsilon_{011}v_{3d}^M + \epsilon_{012}\bar{v}_{3d}^M)\|\boldsymbol{v} - \boldsymbol{v}_d\|_{L^2}^2 + \Big(\tfrac{m_0 v_{3d}^M}{4\epsilon_{011}} + \tfrac{|J_{01} - J_{02}|\omega_{3d}^M}{2}\Big)\big\langle 1, \omega_1^2 + \omega_2^2\big\rangle_{L^2} + J_{03}\bar{\omega}_{3d}^M\epsilon_{014}\big\langle 1, (\omega_3 - \omega_{3d})^2\big\rangle_{L^2}\\
&+\Big((G\bar{A}_1 \vee G\bar{A}_2)v_{3d}^M\epsilon_{013} + \tfrac{|G\bar{A}_1 - G\bar{A}_2|\omega_{3d}^M}{2}\Big)\big\langle 1, \eta_1^2 + \eta_2^2\big\rangle_{L^2} + \tfrac{(G\bar{A}_1 \vee G\bar{A}_2)v_{3d}^M}{4\epsilon_{013}}\big\langle 1, \mu_1^2 + \mu_2^2\big\rangle_{L^2} + \tfrac{m_0\Gamma|\bar{v}_{3d}^M}{4\epsilon_{012}} + \tfrac{J_{03}\Gamma\bar{\omega}_{3d}^M}{4\epsilon_{014}}\\
&+\big\langle \boldsymbol{v} - \boldsymbol{v}_d, \boldsymbol{f}_1\big\rangle_{L^2} + \big\langle \boldsymbol{\omega} - \boldsymbol{\omega}_d, \boldsymbol{f}_2\big\rangle_{L^2},
\end{aligned} \tag{47}$$

where $\epsilon_{01i}, i = 1, ..., 4$ are positive constants to be specified. It is clearly seen from (47) that the energy of the beam does not conserve due to the terms multiplied by v_{3d}^M, $\bar{v}_{3d}^M$, ω_{3d}^M, and $\bar{\omega}_{3d}^M$.

Calculation of $\mathcal{L}U_1$: Since this is a complicated and difficult task in the control design, details are given. We use the fact that $\big\langle \boldsymbol{\vartheta}, \boldsymbol{v}s\big\rangle_{L^2} = \big\langle \boldsymbol{R}_1(\boldsymbol{q})\boldsymbol{\vartheta}, \tilde{\boldsymbol{r}}_t s\big\rangle_{L^2}$ because of (7) and then differentiate U_1 given in (37) along the solutions of (34) to obtain:

$$\mathcal{L}U_1 = A_1 + A_2 + A_3 + B_1 + B_2 + B_3 + \gamma\big\langle (\mathbb{D}\boldsymbol{r} - \varrho\boldsymbol{R}_1(\boldsymbol{q})\mathbb{D}\boldsymbol{r}^0), \boldsymbol{R}_1(\boldsymbol{q})\boldsymbol{f}_1 s\big\rangle_{L^2} + \gamma\big\langle \boldsymbol{\mu}, \boldsymbol{f}_2 s\big\rangle_{L^2}, \tag{48}$$

where

$$\begin{aligned}
A_1 &= \gamma m_0\big\langle \mathbb{D}\boldsymbol{r}_t - \varrho\boldsymbol{R}_{1t}(\boldsymbol{q})\mathbb{D}\boldsymbol{r}^0, \boldsymbol{R}_1(\boldsymbol{q})(\boldsymbol{v} - \boldsymbol{v}_d)s\big\rangle_{L^2},\\
A_2 &= -\gamma m_0\big\langle (\mathbb{D}\boldsymbol{r} - \varrho\boldsymbol{R}_1(\boldsymbol{q})\mathbb{D}\boldsymbol{r}^0), (\boldsymbol{R}_{1t}(\boldsymbol{q})\boldsymbol{v}_d + \boldsymbol{R}_1(\boldsymbol{q})\dot{v}_d)s\big\rangle_{L^2},\\
A_3 &= \gamma\big\langle (\mathbb{D}\boldsymbol{r} - \varrho\boldsymbol{R}_1(\boldsymbol{q})\mathbb{D}\boldsymbol{r}^0), \mathbb{D}\boldsymbol{n}s\big\rangle_{L^2},\\
B_1 &= \gamma\big\langle \mathbb{D}\boldsymbol{\omega}, \boldsymbol{J}_0(\boldsymbol{\omega} - \boldsymbol{\omega}_d)s\big\rangle_{L^2} + \gamma\big\langle \boldsymbol{\mu}, \mathbb{D}\boldsymbol{m}s\big\rangle_{L^2} + \gamma\big\langle \boldsymbol{\mu}, \mathbb{D}\boldsymbol{r}\times\boldsymbol{n}\big\rangle_{L^2},\\
B_2 &= \gamma\big\langle \boldsymbol{\omega}\times\boldsymbol{\mu}, \boldsymbol{J}_0(\boldsymbol{\omega} - \boldsymbol{\omega}_d)s\big\rangle_{L^2} - \gamma\big\langle \boldsymbol{\mu}, \boldsymbol{\omega}\times\boldsymbol{J}_0\boldsymbol{\omega}\big\rangle_{L^2},\\
B_3 &= -\gamma\big\langle \boldsymbol{\mu}, \boldsymbol{J}_0\dot{\boldsymbol{\omega}}_d s\big\rangle_{L^2},
\end{aligned} \tag{49}$$

where we have used $\boldsymbol{\mu}_t = \mathbb{D}\boldsymbol{\omega} + \boldsymbol{\omega}\times\boldsymbol{\mu}$. We now calculate A_i and B_i, $i = 1, 2, 3$.

Applying integration by parts and Young's inequality to the term A_1 results in

$$\begin{aligned}
A_1 \le\ & \tfrac{\gamma\Gamma m_0}{2}\|\boldsymbol{v}^{B\Gamma} - \boldsymbol{v}_d\|^2 + \tfrac{\gamma\Gamma m_0 v_{3d}^M}{4\epsilon_{11}}\big\langle 1, \mu_1^2 + \mu_2^2\big\rangle_{L^2} + \tfrac{\gamma\varrho\Gamma m_0}{4\epsilon_{12}}\big\langle 1, \omega_1^2 + \omega_2^2\big\rangle_{L^2}\\
&+\Big(-\tfrac{\gamma m_0}{2} + \gamma\Gamma m_0 v_{3d}^M\epsilon_{11} + \gamma\Gamma\varrho m_0\epsilon_{12}\Big)\|\boldsymbol{v} - \boldsymbol{v}_d\|_{L^2}^2,
\end{aligned} \tag{50}$$

where ϵ_{11} and ϵ_{12} are positive constants to be chosen.

Using the first equation of (3) and Young's inequality, the upper-bound of A_2 can be calculated as follows

$$\begin{aligned}
A_2 \le\ & \tfrac{\gamma\Gamma m_0}{4}\Big(\tfrac{v_{3d}^M}{\epsilon_{13}} + \tfrac{\bar{v}_{3d}^M}{\epsilon_{14}}\Big)\|\boldsymbol{\vartheta}\|_{L^2}^2 + \gamma\Gamma m_0 v_{3d}^M\Big(\epsilon_{13} + \tfrac{1-\varrho}{4\epsilon_{15}}\Big)\big\langle 1, \omega_1^2 + \omega_2^2\big\rangle_{L^2}\\
&+\gamma\Gamma^2\Big(\bar{v}_{3d}^M\epsilon_{14} + (1-\varrho)v_{3d}^M\epsilon_{15} + \tfrac{(1-\varrho)\bar{v}_{3d}^M}{2}\Big),
\end{aligned} \tag{51}$$

where ϵ_{13}, ϵ_{14}, and ϵ_{15} are positive constants to be chosen.

Using identity 5) in (30), integration by parts, and Young's inequality, the upper-bound of A_3 is calculated as follows

$$\begin{aligned}
A_3 \le\ & \gamma\Gamma\boldsymbol{n}^{B\Gamma}(\mathbb{D}\boldsymbol{r}^{B\Gamma} - \varrho\boldsymbol{R}_1(\boldsymbol{q}^{B\Gamma})\mathbb{D}\boldsymbol{r}^0) - \tfrac{\gamma\Gamma}{2}(G\bar{A}_1 \wedge G\bar{A}_2 \wedge EA)\|\boldsymbol{\vartheta}^{B\Gamma}\|^2 + \tfrac{\varrho\gamma\Gamma(G\bar{A}_1 \vee G\bar{A}_2)}{4\epsilon_{16}}\big\langle 1, \mu_1^2 + \mu_2^2\big\rangle_{L^2}\\
&-\gamma\Big(\big(\tfrac{G\bar{A}_1 \wedge G\bar{A}_2}{2} - \varrho\Gamma\epsilon_{16}(G\bar{A}_1 \vee G\bar{A}_2)\big) \wedge \tfrac{EA}{2}\Big)\|\boldsymbol{\vartheta}\|_{L^2}^2 - \gamma\big\langle \boldsymbol{n}, (\boldsymbol{\mu}\times\mathbb{D}\boldsymbol{r})s\big\rangle_{L^2},
\end{aligned} \tag{52}$$

where ϵ_{16} is a positive constant to be chosen.

Applying integration by parts and Young's inequality to the term B_1 results in

$$\begin{aligned}B_1 \leq\ & \tfrac{\gamma\Gamma\lambda_M(\boldsymbol{J}_0)}{2}\|\boldsymbol{\omega}^{B\Gamma}-\boldsymbol{\omega}_d\|^2+\gamma\Gamma(\boldsymbol{m}^{B\Gamma})^T\boldsymbol{\mu}^{B\Gamma}-\tfrac{\gamma\lambda_m(\boldsymbol{J}_0)}{2}\|\boldsymbol{\omega}-\boldsymbol{\omega}_d\|_{L^2}^2-\tfrac{\gamma\Gamma}{3}(EI_1\wedge EI_2\wedge GI_3)\|\boldsymbol{\mu}^{B\Gamma}\|^2\\ &-\tfrac{\gamma\Gamma}{24}(EI_1\wedge EI_2\wedge GI_3)((\mu_1^{B\Gamma})^4+(\mu_2^{B\Gamma})^4+(\mu_3^{B\Gamma})^4)-\tfrac{\gamma}{6}(EI_1\wedge EI_2\wedge GI_3)\|\boldsymbol{\mu}\|_{L^2}^2\\ &-\tfrac{\gamma}{6}(EI_1\wedge EI_2\wedge GI_3)\big\langle 1,\mu_1^4+\mu_2^4+\mu_3^4\big\rangle_{L^2}+\gamma\big\langle\boldsymbol{\mu},\mathbb{D}\boldsymbol{r}\times\boldsymbol{n}\big\rangle_{L^2},\end{aligned}\tag{53}$$

where we have used the fact that $-\frac{1}{2}x^2+\frac{1}{6}x^3-\frac{1}{12}x^4\leq-\frac{1}{3}x^2-\frac{1}{24}x^4$ and $-\frac{1}{2}x^2+\frac{1}{3}x^3-\frac{1}{4}x^4\leq-\frac{1}{6}x^2-\frac{1}{6}x^4$ for all $x\in\mathbb{R}$. Since $\gamma\big\langle\boldsymbol{\mu},\boldsymbol{\omega}\times\boldsymbol{J}_0\boldsymbol{\omega}\big\rangle_{L^2}=\gamma\big\langle\boldsymbol{\mu},\boldsymbol{\omega}\times\boldsymbol{J}_0(\boldsymbol{\omega}-\boldsymbol{\omega}_d\big\rangle_{L^2}+\gamma\big\langle\boldsymbol{\mu},\boldsymbol{\omega}\times\boldsymbol{J}_0\boldsymbol{\omega}_d\big\rangle_{L^2}$, by using Young's inequality the upper-bound of B_2 can be calculated as

$$\begin{aligned}B_2\leq\ & \gamma\Gamma\tilde{J}_{0M}\epsilon_{21}\|\boldsymbol{\mu}\|_{L^2}^2+\tfrac{\gamma\Gamma\tilde{J}_{0M}}{\epsilon_{21}}\big\langle 1,\omega_1^4+\omega_2^4+(\omega_3-\omega_{3d})^4\big\rangle_{L^2}+\tfrac{2\gamma\Gamma\omega_{3d}^M\lambda_M(\boldsymbol{J}_0)}{\epsilon_{22}}\big\langle 1,\omega_1^2+\omega_2^2\big\rangle_{L^2}\\ &+2\gamma\Gamma\omega_{3d}^M\lambda_M(J_0)\epsilon_{22}\big\langle 1,\mu_1^2+\mu_2^2\big\rangle_{L^2},\end{aligned}\tag{54}$$

where ϵ_{21} and ϵ_{22} are positive constants to be specified.

Applying Young's inequality to the term B_3 results in

$$B_3\leq\gamma\Gamma\bar{\omega}_{3d}^M J_{03}\epsilon_{23}\|\mu_3\|_{L^2}^2+\tfrac{\gamma\Gamma^2\bar{\omega}_{3d}^M J_{03}}{4\epsilon_{23}},\tag{55}$$

where ϵ_{23} is a positive constant to be chosen. Substituting (50), (50), (51), (52), (53), (53), and (55) into (48) yields

$$\begin{aligned}\mathcal{L}U_1\leq\ & \tfrac{\gamma\Gamma m_0}{2}\|\boldsymbol{v}^{B\Gamma}-\boldsymbol{v}_d\|^2+\gamma\Gamma(\boldsymbol{n}^{B\Gamma})^T(\mathbb{D}\boldsymbol{r}^{B\Gamma}-\varrho\boldsymbol{R}_1(\boldsymbol{q}^{B\Gamma})\mathbb{D}\boldsymbol{r}^0)-\tfrac{\gamma\Gamma}{2}(G\bar{A}_1\wedge G\bar{A}_2\wedge EA)\|\boldsymbol{\vartheta}^{B\Gamma}\|^2\\ &+\tfrac{\gamma\Gamma\lambda_M(\boldsymbol{J}_0)}{2}\|\boldsymbol{\omega}^{B\Gamma}-\boldsymbol{\omega}_d\|^2+\gamma\Gamma(\boldsymbol{m}^{B\Gamma})^T\boldsymbol{\mu}^{B\Gamma}-\tfrac{\gamma\Gamma}{3}(EI_1\wedge EI_2\wedge GI_3)\|\boldsymbol{\mu}^{B\Gamma}\|^2\\ &-\tfrac{\gamma\Gamma}{24}(EI_1\wedge EI_2\wedge GI_3)((\mu_1^{B\Gamma})^4+(\mu_2^{B\Gamma})^4+(\mu_3^{B\Gamma})^4)+\Big[-\tfrac{\gamma m_0}{2}+\gamma\Gamma m_0 v_{3d}^M\epsilon_{11}+\gamma\Gamma\varrho m_0\epsilon_{12}\Big]\|\boldsymbol{v}-\boldsymbol{v}_d\|_{L^2}^2\\ &+\Big[-\tfrac{\gamma\lambda_m(\boldsymbol{J}_0)}{2}+\tfrac{\gamma\varrho\Gamma m_0}{4\epsilon_{12}}+\gamma\Gamma m_0 v_{3d}^M\Big(\epsilon_{13}+\tfrac{1-\varrho}{4\epsilon_{15}}\Big)+\tfrac{2\gamma\Gamma\omega_{3d}^M\lambda_M(\boldsymbol{J}_0)}{\epsilon_{22}}\Big]\|\boldsymbol{\omega}-\boldsymbol{\omega}_d\|^2+\tfrac{\gamma\Gamma\tilde{J}_{0M}}{\epsilon_{21}}\big\langle 1,\omega_1^4+\omega_2^4+(\omega_3-\omega_{3d})^4\big\rangle_{L^2}\\ &-\gamma\Big[\Big(\big(\tfrac{G\bar{A}_1\wedge G\bar{A}_2}{2}-\varrho\Gamma\epsilon_{16}(G\bar{A}_1\vee G\bar{A}_2)\big)\wedge\tfrac{EA}{2}\Big)-\tfrac{\Gamma m_0}{4}\Big(\tfrac{v_{3d}^M}{\epsilon_{13}}+\tfrac{\bar{v}_{3d}^M}{\epsilon_{14}}\Big)\Big]\|\boldsymbol{\vartheta}\|_{L^2}^2\\ &-\gamma\Big[\Big(\tfrac{1}{6}(EI_1\wedge EI_2)-\tfrac{\Gamma m_0 v_{3d}^M}{4\epsilon_{11}}-\tfrac{\varrho\Gamma(G\bar{A}_1\vee G\bar{A}_2)}{4\epsilon_{16}}-2\Gamma\omega_{3d}^M\lambda_M(J_0)\epsilon_{22}\Big)\wedge\Big(GI_3-\Gamma\bar{\omega}_{3d}^M J_{03}\epsilon_{23}\Big)\Big]\|\boldsymbol{\mu}\|_{L^2}^2\\ &-\tfrac{\gamma}{6}(EI_1\wedge EI_2\wedge GI_3)\big\langle 1,\mu_1^4+\mu_2^4+\mu_3^4\big\rangle_{L^2}+\gamma\Gamma^2\Big(\bar{v}_{3d}^M\epsilon_{14}+(1-\varrho)v_{3d}^M\epsilon_{15}+\tfrac{(1-\varrho)\bar{v}_{3d}^M}{2}\Big)+\tfrac{\gamma\Gamma^2\bar{\omega}_{3d}^M J_{03}}{4\epsilon_{23}}\\ &+\gamma\big\langle(\mathbb{D}\boldsymbol{r}-\varrho\boldsymbol{R}_1(\boldsymbol{q})\mathbb{D}\boldsymbol{r}^0),\boldsymbol{R}_1(\boldsymbol{q})\boldsymbol{f}_1 s\big\rangle_{L^2}+\gamma\big\langle\boldsymbol{\mu},\boldsymbol{f}_2 s\big\rangle_{L^2}.\end{aligned}\tag{56}$$

Calculation of $\mathcal{L}U_B$: Differentiating U_B given in (37) along the solutions of (35)gives

$$\begin{aligned}\mathcal{L}U_B=\ & (v_3^{B0}-v_{3d})(N^{B0}+f_1^{B0})+(\omega_3^{B0}-\omega_{3d})(T^{B0}+f_2^{B0})+\big[\gamma_1(\tilde{\boldsymbol{r}}_1^{B\Gamma}-\tilde{\boldsymbol{r}}_d)+\boldsymbol{R}_1(\boldsymbol{q}^{B\Gamma})(\boldsymbol{v}^{B\Gamma}-\boldsymbol{v}_d)\\ &+\gamma\Gamma\boldsymbol{R}_1(\boldsymbol{q}^{B\Gamma})\boldsymbol{\vartheta}^{B\Gamma}\big]^T\big[\gamma_1\boldsymbol{M}_H(\tilde{\boldsymbol{r}}_2^{B\Gamma}-\dot{\tilde{\boldsymbol{r}}}_d)-\boldsymbol{n}^{B\Gamma}+\boldsymbol{\phi}_{1B}+\boldsymbol{f}_1^{B\Gamma}-\boldsymbol{M}_H\dot{\boldsymbol{R}}_1(\boldsymbol{q}^{B\Gamma})\boldsymbol{v}_d-\boldsymbol{M}_H\boldsymbol{R}_1(\boldsymbol{q}^{B\Gamma})\dot{\boldsymbol{v}}_d\\ &+\gamma\Gamma\boldsymbol{M}_H\dot{\boldsymbol{R}}_1(\boldsymbol{q}^{B\Gamma})\boldsymbol{\vartheta}^{B\Gamma}+\gamma\Gamma\boldsymbol{M}_H\boldsymbol{R}_1(\boldsymbol{q}^{B\Gamma})\dot{\boldsymbol{\vartheta}}^{B\Gamma}\big]+2\gamma_1 k_{1B}(\tilde{\boldsymbol{r}}_1^{B\Gamma}-\tilde{\boldsymbol{r}}_d)^T(\tilde{\boldsymbol{r}}_2^{B\Gamma}-\dot{\tilde{\boldsymbol{r}}}_d)\\ &+\big[\gamma_2\boldsymbol{G}^T\bar{\boldsymbol{\xi}}+\boldsymbol{\omega}^{B\Gamma}-\boldsymbol{\omega}_d+\gamma\Gamma\boldsymbol{\mu}^{B\Gamma}\big]^T\big[\gamma_2\boldsymbol{J}_H\dot{\boldsymbol{G}}^T\bar{\boldsymbol{\xi}}+\gamma_2\boldsymbol{J}_H\boldsymbol{G}^T\dot{\bar{\boldsymbol{\xi}}}-\boldsymbol{m}^{B\Gamma}-\boldsymbol{\omega}^{B\Gamma}\times(\boldsymbol{J}_H\boldsymbol{\omega}^{B\Gamma})\\ &+\boldsymbol{\phi}_{2B}+\boldsymbol{f}_2^{B\Gamma}-\boldsymbol{J}_H\dot{\boldsymbol{\omega}}_d+\gamma\Gamma\dot{\boldsymbol{\mu}}^{B\Gamma}\big]+2\gamma_2 k_{2B}\bar{\boldsymbol{\xi}}^T\boldsymbol{G}(\boldsymbol{\omega}^{B\Gamma}-\boldsymbol{\omega}_d).\end{aligned}\tag{57}$$

Since $(\boldsymbol{n}^{B0})^T\boldsymbol{R}_1(\boldsymbol{q}^{B0})(\boldsymbol{v}^{B0}-\boldsymbol{v}_d)=N^{B0}(v_3^{B0}-v_{3d})$ and $(\boldsymbol{m}^{B0})^T(\boldsymbol{\omega}^{B0}-\boldsymbol{\omega}_d)=T^{B0}(\omega_3^{B0}-\omega_{3d})$ due to the boundary conditions in (35), the expression of $\mathcal{L}U_0$ in (47), $\mathcal{L}U_1$ in (56), and $\mathcal{L}U_B$ in (57) suggests that we choose the boundary controls $\boldsymbol{\phi}_{1B}$ and $\boldsymbol{\phi}_{2B}$ as follows

$$\begin{aligned}\boldsymbol{\phi}_{1B}=\ & -\big(k_{1B}+\epsilon_{11B}+\epsilon_{12B}\big)\big(\gamma_1(\tilde{\boldsymbol{r}}_1^{B\Gamma}-\tilde{\boldsymbol{r}}_d)+\boldsymbol{R}_1(\boldsymbol{q}^{B\Gamma})(\boldsymbol{v}^{B\Gamma}-\boldsymbol{v}_d)+\gamma\Gamma\boldsymbol{R}_1(\boldsymbol{q}^{B\Gamma})\boldsymbol{\vartheta}^{B\Gamma}\big)-\gamma_1\boldsymbol{M}_H(\tilde{\boldsymbol{r}}_2^{B\Gamma}-\dot{\tilde{\boldsymbol{r}}}_d)\\ &-\boldsymbol{R}_1(\boldsymbol{q}^{B\Gamma})\boldsymbol{D}_{11}^{\Gamma}\boldsymbol{v}^{B\Gamma}+\boldsymbol{M}_H\dot{\boldsymbol{R}}_1(\boldsymbol{q}^{B\Gamma})\boldsymbol{v}_d+\boldsymbol{M}_H\boldsymbol{R}_1(\boldsymbol{q}^{B\Gamma})\dot{\boldsymbol{v}}_d-\gamma\Gamma\boldsymbol{M}_H\dot{\boldsymbol{R}}_1(\boldsymbol{q}^{B\Gamma})\boldsymbol{\vartheta}^{B\Gamma}-\gamma\Gamma\boldsymbol{M}_H\boldsymbol{R}_1(\boldsymbol{q}^{B\Gamma})\dot{\boldsymbol{\vartheta}}^{B\Gamma},\\ \boldsymbol{\phi}_{2B}=\ & -\big(k_{2B}+\epsilon_{21B}+\epsilon_{22B}\big)\big(\gamma_2\boldsymbol{G}^T\bar{\boldsymbol{\xi}}+\boldsymbol{\omega}^{B\Gamma}-\boldsymbol{\omega}_d+\gamma\Gamma\boldsymbol{\mu}^{B\Gamma}\big)-\gamma_2\boldsymbol{J}_H\dot{\boldsymbol{G}}^T\bar{\boldsymbol{\xi}}-\gamma_2\boldsymbol{J}_H\boldsymbol{G}^T\dot{\bar{\boldsymbol{\xi}}}+\boldsymbol{\omega}^{B\Gamma}\times(\boldsymbol{J}_H\boldsymbol{\omega}^{B\Gamma})\\ &+\boldsymbol{D}_{21}^{\Gamma}\boldsymbol{\omega}^{B\Gamma}+\boldsymbol{D}_{22}^{\Gamma}(\boldsymbol{\omega}\otimes\boldsymbol{\omega}^{B\Gamma})\boldsymbol{\omega}^{B\Gamma}+\boldsymbol{J}_H\dot{\boldsymbol{\omega}}_d-\gamma\Gamma\dot{\boldsymbol{\mu}}^{B\Gamma},\end{aligned}\tag{58}$$

where ϵ_{ijB}, $(i,\,j)=1,\,2$ are positive constants. It is seen from (58) that the boundary control vectors $\boldsymbol{\phi}_{iB}$, $i=1,\,2$ require only full states of the beam at the actuated end and the reference states, i.e., these control vectors are boundary state-feedback.

Remark 4.2: *Since $\dot{\boldsymbol{R}}_1(\boldsymbol{q}^{B\Gamma})=\frac{\partial\boldsymbol{R}_1(\boldsymbol{q}^{B\Gamma})}{\partial\boldsymbol{q}^{B\Gamma}}\boldsymbol{K}(\boldsymbol{q}^{B\Gamma})\boldsymbol{\omega}^{B\Gamma}$, only measurements from the actuated end of the beam are required for implementation of the boundary controls $\boldsymbol{\phi}_{1B}$ and $\boldsymbol{\phi}_{2B}$. The terms $\tilde{\boldsymbol{r}}_1^{B\Gamma}$ and $\boldsymbol{q}^{B\Gamma}$ can be measured by using translational and rotational displacement sensors ($\boldsymbol{q}^{B\Gamma}$ is determined from Euler angles via the relationship (8)). The terms $\boldsymbol{\vartheta}^{B\Gamma}$ and $\boldsymbol{\mu}^{B\Gamma}$ can be measured by using strain gauges. The terms $\tilde{\boldsymbol{r}}_2^{B\Gamma}$, $\boldsymbol{\omega}^{B\Gamma}$, $\dot{\boldsymbol{\vartheta}}^{B\Gamma}$, and $\dot{\boldsymbol{\mu}}^{B\Gamma}$ can be obtained by using band-pass filters, through which*

the measurements of $\tilde{\boldsymbol{r}}_1^{B\Gamma}$, $\boldsymbol{q}^{B\Gamma}$, $\boldsymbol{\vartheta}^{B\Gamma}$, *and* $\boldsymbol{\mu}^{B\Gamma}$ *are passed, respectively. Then* $\boldsymbol{v}^{B\Gamma}=\boldsymbol{R}_1^{-1}(\boldsymbol{q}^{B\Gamma})\boldsymbol{r}_2^{B\Gamma}$, *see (7).*

Substituting $\mathcal{L}U_0$ in (47), $\mathcal{L}U_1$ in (56), and $\mathcal{L}U_B$ in (57) together with the boundary controls $\boldsymbol{\phi}_{1B}$ and $\boldsymbol{\phi}_{2B}$ in (58) into (44) results in

$$\begin{aligned}\mathcal{L}U \leq\ & k_{11}^{\diamond}\|\boldsymbol{v}-\boldsymbol{v}_d\|_{L^2}^2+k_{12}^{\diamond}\|\boldsymbol{\omega}-\boldsymbol{\omega}_d\|_{L^2}^2+k_{12N}^{\diamond}\big\langle 1,\omega_1^4+\omega_2^4+(\omega_3-\omega_{3d})^4\big\rangle_{L^2}\\ & -k_{21}^{\diamond}\|\boldsymbol{\vartheta}\|_{L^2}^2-k_{22}^{\diamond}\|\boldsymbol{\mu}\|_{L^2}^2-k_{22N}^{\diamond}\big\langle 1,\mu_1^4+\mu_2^4+\mu_3^4\big\rangle_{L^2}+\Omega+\Omega_B+c_0^{\diamond},\end{aligned}\tag{59}$$

where

$$\begin{aligned}
&k_{11}^{\diamond}=m_0(\epsilon_{011}v_{3d}^M+\epsilon_{012}\bar{v}_{3d}^M)-\tfrac{\gamma m_0}{2}+\gamma\Gamma m_0v_{3d}^M\epsilon_{11}+\gamma\Gamma\varrho m_0\epsilon_{12},\\
&k_{12}^{\diamond}=\big(\tfrac{m_0v_{3d}^M}{4\epsilon_{011}}+\tfrac{|J_{01}-J_{02}|\omega_{3d}^M}{2}\big)\vee J_{03}|\dot{\omega}_{3d}|\epsilon_{014}-\tfrac{\gamma\lambda_m(\boldsymbol{J}_0)}{2}+\tfrac{\gamma\varrho\Gamma m_0}{4\epsilon_{12}}+\gamma\Gamma m_0v_{3d}^M\big(\epsilon_{13}+\tfrac{1-\varrho}{4\epsilon_{15}}\big)+\tfrac{2\gamma\Gamma\omega_{3d}^M\lambda_M(\boldsymbol{J}_0)}{\epsilon_{22}},\\
&k_{12N}^{\diamond}=\tfrac{\gamma\Gamma\tilde{J}_{0M}}{\epsilon_{21}},\\
&k_{21}^{\diamond}=\gamma\big[\big(\big(\tfrac{G\bar{A}_1\wedge G\bar{A}_2}{2}-\varrho\Gamma\epsilon_{16}(G\bar{A}_1\vee G\bar{A}_2)-\tfrac{1}{\gamma}\big((G\bar{A}_1\vee G\bar{A}_2)v_{3d}^M\epsilon_{013}+\tfrac{|G\bar{A}_1-G\bar{A}_2|\omega_{3d}^M}{2}\big)\big)\wedge\tfrac{EA}{2}\big)\\
&\quad-\tfrac{\Gamma m_0}{4}\big(\tfrac{v_{3d}^M}{\epsilon_{13}}+\tfrac{\bar{v}_{3d}^M}{\epsilon_{14}}\big)\big],\\
&k_{22}^{\diamond}=\gamma\big[\big(\tfrac{1}{6}(EI_1\wedge EI_2)-\tfrac{\Gamma m_0v_{3d}^M}{4\epsilon_{11}}-\tfrac{\varrho\Gamma(G\bar{A}_1\vee G\bar{A}_2)}{4\epsilon_{16}}-2\Gamma\omega_{3d}^M\lambda_M(J_0)\epsilon_{22}-\tfrac{(G\bar{A}_1\vee G\bar{A}_2)v_{3d}^M}{4\gamma\epsilon_{013}}\big)\wedge\big(GI_3-\Gamma\bar{\omega}_{3d}^MJ_{03}\epsilon_{23}\big)\big],\\
&k_{22N}^{\diamond}=\tfrac{\gamma}{6}(EI_1\wedge EI_2\wedge GI_3),\\
&c_0^{\diamond}=\tfrac{m_0\Gamma|\dot{v}_{3d}|}{4\epsilon_{012}}+\tfrac{J_{03}\Gamma|\dot{\omega}_{3d}|}{4\epsilon_{014}}+\gamma\Gamma^2\big(\bar{v}_{3d}^M\epsilon_{14}+(1-\varrho)v_{3d}^M\epsilon_{15}+\tfrac{(1-\varrho)\bar{v}_{3d}^M}{2}\big)+\tfrac{\gamma\Gamma^2\bar{\omega}_{3d}^MJ_{03}}{4\epsilon_{23}},
\end{aligned}\tag{60}$$

and

$$\begin{aligned}
\Omega=\ & \big\langle\boldsymbol{v}-\boldsymbol{v}_d,\boldsymbol{f}_1\big\rangle_{L^2}+\big\langle\boldsymbol{\omega}-\boldsymbol{\omega}_d,\boldsymbol{f}_2\big\rangle_{L^2}+\gamma\big\langle(\mathbb{D}\boldsymbol{r}-\varrho\boldsymbol{R}_1(\boldsymbol{q})\mathbb{D}\boldsymbol{r}^0),\boldsymbol{R}_1(\boldsymbol{q})\boldsymbol{f}_1s\big\rangle_{L^2}+\gamma\big\langle\boldsymbol{\mu},\boldsymbol{f}_2s\big\rangle_{L^2},\\
\Omega_B=\ & -\gamma_1(\tilde{\boldsymbol{r}}_1^{B\Gamma}-\tilde{\boldsymbol{r}}_d)^T\boldsymbol{n}^{B\Gamma}+(1-\varrho)\gamma\Gamma(\boldsymbol{R}_1(\boldsymbol{q}^{B\Gamma})\mathbb{D}\boldsymbol{r}^0)^T\boldsymbol{n}^{B\Gamma}-\gamma_2(\boldsymbol{G}^T\bar{\boldsymbol{\xi}})^T\boldsymbol{m}^{B\Gamma}-\tfrac{\gamma\Gamma}{2}(G\bar{A}_1\wedge G\bar{A}_2\wedge EA)\|\boldsymbol{\vartheta}^{B\Gamma}\|^2\\
& -\tfrac{\gamma\Gamma}{3}(EI_1\wedge EI_2\wedge GI_3)\|\boldsymbol{\mu}^{B\Gamma}\|^2-\tfrac{\gamma\Gamma}{24}(EI_1\wedge EI_2\wedge GI_3)((\mu_1^{B\Gamma})^4+(\mu_2^{B\Gamma})^4+(\mu_3^{B\Gamma})^4)\\
& +(v_3^{B0}-v_{3d})f_1^{B0}+(\omega_3^{B0}-\omega_{3d})f_2^{B0}-\big(k_{1B}+\epsilon_{11B}+\epsilon_{12B}\big)\|\gamma_1(\tilde{\boldsymbol{r}}_1^{B\Gamma}-\tilde{\boldsymbol{r}}_d)+\boldsymbol{R}_1(\boldsymbol{q}^{B\Gamma})(\boldsymbol{v}^{B\Gamma}-\boldsymbol{v}_d)\\
& +\gamma\Gamma\boldsymbol{R}_1(\boldsymbol{q}^{B\Gamma})\boldsymbol{\vartheta}^{B\Gamma}\|^2+\big[\gamma_1(\tilde{\boldsymbol{r}}_1^{B\Gamma}-\tilde{\boldsymbol{r}}_d)+\boldsymbol{R}_1(\boldsymbol{q}^{B\Gamma})(\boldsymbol{v}^{B\Gamma}-\boldsymbol{v}_d)+\gamma\Gamma\boldsymbol{R}_1(\boldsymbol{q}^{B\Gamma})\boldsymbol{\vartheta}^{B\Gamma}\big]\boldsymbol{f}_{10}^{B\Gamma}\\
& +2\gamma_1k_{1B}(\tilde{\boldsymbol{r}}_1^{B\Gamma}-\tilde{\boldsymbol{r}}_d)^T(\tilde{\boldsymbol{r}}_2^{B\Gamma}-\dot{\tilde{\boldsymbol{r}}}_d)-\big(k_{2B}+\epsilon_{21B}+\epsilon_{22B}\big)\|\gamma_2\boldsymbol{G}^T\bar{\boldsymbol{\xi}}+\boldsymbol{\omega}^{B\Gamma}-\boldsymbol{\omega}_d+\gamma\Gamma\boldsymbol{\mu}^{B\Gamma}\|^2\\
& +\big[\gamma_2\boldsymbol{G}^T\bar{\boldsymbol{\xi}}+\boldsymbol{\omega}^{B\Gamma}-\boldsymbol{\omega}_d+\gamma\Gamma\boldsymbol{\mu}^{B\Gamma}\big]\boldsymbol{f}_{20}^{B\Gamma}+2\gamma_2k_{2B}\bar{\boldsymbol{\xi}}^T\boldsymbol{G}(\boldsymbol{\omega}^{B\Gamma}-\boldsymbol{\omega}_d).
\end{aligned}\tag{61}$$

It is noted that in order to obtain (59), we have added and subtracted the terms $\gamma_1(\tilde{\boldsymbol{r}}_1^{B\Gamma}-\tilde{\boldsymbol{r}}_d)^T\boldsymbol{n}^{B\Gamma}$ and $\gamma_2(\boldsymbol{G}^T\bar{\boldsymbol{\xi}})^T\boldsymbol{m}^{B\Gamma}$ to $\mathcal{L}U_B$. We now calculate the upper-bound of Ω and Ω_B. Using the expression of $\boldsymbol{f}_1$ and $\boldsymbol{f}_2$, see (6), Young's inequality, and the identity $(x-x_d)^3=x^3-3x_d(x-x_d)^2-3x_d^2(x-x_d)-x_d^3$ for all $(x,x_d)\in\mathbb{R}$, the upper-bound of Ω can be calculated as follows

$$\begin{aligned}\Omega\leq\ & -k_{11}^*\|\boldsymbol{v}-\boldsymbol{v}_d\|_{L^2}^2-k_{12}^*\|\boldsymbol{\omega}-\boldsymbol{\omega}_d\|_{L^2}^2-k_{12N}^*\big\langle 1,\omega_1^4+\omega_2^4+(\omega_3-\omega_{3d})^4\big\rangle_{L^2}+k_{21}^*\|\boldsymbol{\vartheta}\|_{L^2}^2\\ & +k_{22}^*\|\boldsymbol{\mu}\|_{L^2}^2+k_{22N}^*\big\langle 1,\mu_1^4+\mu_2^4+\mu_3^4\big\rangle_{L^2}+c_0^*,\end{aligned}\tag{62}$$

where

$$\begin{aligned}
&k_{11}^*=\lambda_m(\boldsymbol{D}_{11})-\lambda_M(\boldsymbol{D}_11)v_{3d}^M\delta_{01}-\delta_{02}-\tfrac{\gamma\Gamma\lambda_M(\boldsymbol{D}_{11})}{4\delta_{11}}-\gamma(1-\varrho)\Gamma\lambda_M(\boldsymbol{D}_{11})\delta_{14},\\
&k_{12}^*=\lambda_m(\boldsymbol{D}_{21})-\lambda_M(\boldsymbol{D}_{21})\omega_{3d}^M\delta_{03}-\delta_{04}-\tfrac{\gamma\Gamma\lambda_M(\boldsymbol{D}_{21})}{4\delta_{21}}-\tfrac{3\gamma\Gamma(\omega_{3d}^M)^2}{4\delta_{15}},\\
&k_{12N}^*=\lambda_m(\boldsymbol{D}_{22})-\tfrac{\omega_{3d}^M\delta_{05}^{4/3}}{4}-3(\omega_{3d}^M)^2\delta_{06}-\tfrac{(\omega_{3d}^M)^3\delta_{07}^4}{4}-\tfrac{3\gamma\Gamma\lambda_M(\boldsymbol{D}_{22})}{4\delta_{23}^{4/3}}-\tfrac{\gamma\Gamma\omega_{3d}^M\lambda_M(\boldsymbol{D}_{22})}{4\delta_{24}},\\
&k_{21}^*=\gamma\Gamma(\lambda_M(\boldsymbol{D}_{11})(\delta_{11}+v_{3d}^M\delta_{12})+\delta_{13}),\\
&k_{22}^*=\gamma\Gamma\lambda_M(\boldsymbol{D}_{21})\delta_{21}+\gamma\Gamma\omega_{3d}^M\lambda_M(\boldsymbol{D}_{21})\delta_{22}+\gamma\Gamma\omega_{3d}^M\lambda_M(\boldsymbol{D}_{22})\delta_{24}+3\gamma\Gamma(\omega_{3d}^M)^2\lambda_M(\boldsymbol{D}_{22})\delta_{25}\\
&\quad+\gamma\Gamma\omega_{3d}^M\lambda_M(\boldsymbol{D}_{22})\delta_{26}+\gamma\Gamma\delta_{27},\\
&k_{22N}^*=\tfrac{\gamma\Gamma\lambda_M(\boldsymbol{D}_{22})\delta_{23}^4}{4},\\
&c_0^*=\tfrac{\lambda_M(\boldsymbol{D}_{11})v_{3d}^M\Gamma}{4\delta_{01}}+\tfrac{\lambda_M(\boldsymbol{D}_{21})\omega_{3d}^M\Gamma}{4\delta_{03}}+\tfrac{3\omega_{3d}^M\Gamma}{4\delta_{05}^4}+\tfrac{3(\omega_{3d}^M)^2\Gamma}{4\delta_{06}}+\tfrac{3(\omega_{3d}^M)^3\Gamma}{4\delta_{07}}+\tfrac{\gamma\lambda_M(\boldsymbol{D}_{11})v_{3d}^M}{4\delta_{12}}+\gamma(1-\varrho)\lambda_M(\boldsymbol{D}_{11})v_{3d}^M\Gamma^2\\
&\quad+\tfrac{\gamma\Gamma^2\omega_{3d}^M\lambda_M(\boldsymbol{D}_{21})}{4\delta_{22}}+\tfrac{\gamma\Gamma^2(\omega_{3d}^M)^3\lambda_M(\boldsymbol{D}_{22})}{4\delta_{26}}+\big(\tfrac{1}{4\delta_{02}}+\tfrac{\gamma\Gamma}{4\delta_{13}}\big)\|\boldsymbol{f}_{10}\|_{L^2}^2+\gamma(1-\varrho)\Gamma|\big\langle 1,\boldsymbol{f}_{10}\big\rangle_{L^2}|+\big(\tfrac{1}{4\delta_{04}}+\tfrac{\gamma\Gamma}{4\delta_{27}}\big)\|\boldsymbol{f}_{20}\|_{L^2},
\end{aligned}\tag{63}$$

with $\delta_{1i},i=1,2,3$ and $\delta_{2i},i=1,...,7$ being positive constants to be chosen. Using the expression of

$\boldsymbol{n}$, $\boldsymbol{m}$, f_1^{B0}, f_2^{B0}, $\boldsymbol{f}_1^{B\Gamma}$, and $\boldsymbol{f}_2^{B\Gamma}$, see (12), (13), and (16), Young's inequality, and expansion of the terms $\|\gamma_1(\tilde{\boldsymbol{r}}_1^{B\Gamma}-\tilde{\boldsymbol{r}}_d)+\boldsymbol{R}_1(\boldsymbol{q}^{B\Gamma})(\boldsymbol{v}^{B\Gamma}-\boldsymbol{v}_d)+\gamma\Gamma\boldsymbol{R}_1(\boldsymbol{q}^{B\Gamma})\boldsymbol{\vartheta}^{B\Gamma}\|^2$ and $\|\gamma_2\boldsymbol{G}^T\bar{\boldsymbol{\xi}}+\boldsymbol{\omega}^{B\Gamma}-\boldsymbol{\omega}_d+\gamma\Gamma\boldsymbol{\mu}^{B\Gamma}\|^2$, we can bound Ω_B as follows

$$\begin{aligned}\Omega_B \le\ & -c_{11B}(v_3^{B0}-v_{3d})^2-c_{12B}(\omega_3^{B0}-\omega_{3d})^2-c_{12NB}(\omega_3^{B0}-\omega_{3d})^4-c_{21B}\|\boldsymbol{\vartheta}^{B\Gamma}\|^2-c_{22B}\|\boldsymbol{\mu}^{B\Gamma}\|^2\\ & -c_{22NB}(\mu_1^4+\mu_2^4+\mu_3^4)-c_{31B}\|\gamma_1(\tilde{\boldsymbol{r}}_1^{B\Gamma}-\tilde{\boldsymbol{r}}_d)+\boldsymbol{R}_1(\boldsymbol{q}^{B\Gamma})(\boldsymbol{v}^{B\Gamma}-\boldsymbol{v}_d)+\gamma\Gamma\boldsymbol{R}_1(\boldsymbol{q}^{B\Gamma})\boldsymbol{\vartheta}^{B\Gamma}\|^2-c_{32B}\|\tilde{\boldsymbol{r}}_1^{B\Gamma}-\tilde{\boldsymbol{r}}_d\|^2\\ & -c_{41B}\|\gamma_2\boldsymbol{G}^T\bar{\boldsymbol{\xi}}+\boldsymbol{\omega}^{B\Gamma}-\boldsymbol{\omega}_d+\gamma\Gamma\boldsymbol{\mu}^{B\Gamma}\|^2-c_{42B}\xi_1^2\|\bar{\boldsymbol{\xi}}\|^2-c_{51B}\|\boldsymbol{v}^{B\Gamma}-\boldsymbol{v}_d\|^2-c_{52B}\|\boldsymbol{\omega}^{B\Gamma}-\boldsymbol{\omega}_d\|^2+c_{0B},\end{aligned} \tag{64}$$

where

$$\begin{aligned}
&c_{11B}=d_{11}^0-d_{11}^0v_{3d}^M\delta_{31}-\delta_{32},\\
&c_{12B}=d_{21}^0-d_{21}^0\omega_{3d}^M\delta_{33}-\delta_{34},\\
&c_{12NB}=d_{22}^0-\tfrac{9d_{22}^0\omega_{3d}^M\delta_{35}^{4/3}}{4}-3d_{22}^0(\omega_{3d}^M)^2\delta_{36}-\tfrac{d_{22}^0(\omega_{3d}^M)^3\delta_{37}^4}{4},\\
&c_{21B}=\tfrac{\gamma\Gamma}{2}(G\bar{A}_1\wedge G\bar{A}_2\wedge EA)+k_{1B}\gamma^2\Gamma^2-\tfrac{k_{1B}\gamma\gamma_1\Gamma}{4\delta_{41}}-\tfrac{k_{1B}\gamma\Gamma}{4\delta_{42}},\\
&c_{22B}=\tfrac{\gamma\Gamma}{3}(EI_1\wedge EI_2\wedge GI_3)+k_{2B}\gamma^2\Gamma^2-\tfrac{k_{2B}\gamma\gamma_2\Gamma}{4\delta_{43}}-\tfrac{k_{2B}\gamma\Gamma}{4\delta_{44}},\\
&c_{22NB}=\tfrac{\gamma\Gamma}{24}(EI_1\wedge EI_2\wedge GI_3),\\
&c_{31B}=\epsilon_{11B},\\
&c_{32B}=k_{1B}\gamma_1^2-k_{1B}\gamma\gamma_1\Gamma\delta_{41},\\
&c_{41B}=\epsilon_{21B},\\
&c_{42B}=k_{2B}\gamma_2^2-k_{2B}\gamma\gamma_2\Gamma\delta_{43},\\
&c_{51B}=k_{1B}-k_{1B}\gamma\Gamma\delta_{42},\\
&c_{52B}=k_{2B}-k_{2B}\gamma\Gamma\delta_{44},\\
&c_{0B}=\tfrac{d_{11}^0v_{3d}^M}{4\delta_{31}}+\tfrac{(f_{10}^{B0})^2}{4\delta_{32}}+\tfrac{d_{21}^0\omega_{3d}^M}{4\delta_{33}}+\tfrac{(f_{20}^{B0})^2}{4\delta_{34}}+\tfrac{3d_{22}^0\omega_{3d}^M}{4\delta_{35}^4}+\tfrac{3d_{22}^0(\omega_{3d}^M)^2}{4\delta_{36}}+\tfrac{3d_{22}^0(\omega_{3d}^M)^3}{4\delta_{37}^{4/3}}+\tfrac{\|\boldsymbol{f}_1^{B\Gamma}\|^2}{4\epsilon_{12B}}+\tfrac{\|\boldsymbol{f}_2^{B\Gamma}\|^2}{4\epsilon_{22B}},
\end{aligned} \tag{65}$$

with $\delta_{3i}, i=1,...,7$ and $\delta_{4i}, i=1,...,4$ being positive constants to be specified. Now, substituting (62) and (64) into (59) results in

$$\begin{aligned}\mathcal{L}U \le\ & -k_{11}\|\boldsymbol{v}-\boldsymbol{v}_d\|_{L^2}^2-k_{12}\|\boldsymbol{\omega}-\boldsymbol{\omega}_d\|_{L^2}^2-k_{12N}\big\langle 1,\omega_1^4+\omega_2^4+(\omega_3-\omega_{3d})^4\big\rangle_{L^2}-k_{21}\|\boldsymbol{\vartheta}\|_{L^2}^2-k_{22}\|\boldsymbol{\mu}\|_{L^2}^2\\ & -k_{22N}\big\langle 1,\mu_1^4+\mu_2^4+\mu_3^4\big\rangle_{L^2}-c_{11B}(v_3^{B0}-v_{3d})^2-c_{12B}(\omega_3^{B0}-\omega_{3d})^2-c_{12NB}(\omega_3^{B0}-\omega_{3d})^4-c_{21B}\|\boldsymbol{\vartheta}^{B\Gamma}\|^2\\ & -c_{22B}\|\boldsymbol{\mu}^{B\Gamma}\|^2-c_{22NB}(\mu_1^4+\mu_2^4+\mu_3^4)-c_{31B}\|\gamma_1(\tilde{\boldsymbol{r}}_1^{B\Gamma}-\tilde{\boldsymbol{r}}_d)+\boldsymbol{R}_1(\boldsymbol{q}^{B\Gamma})(\boldsymbol{v}^{B\Gamma}-\boldsymbol{v}_d)+\gamma\Gamma\boldsymbol{R}_1(\boldsymbol{q}^{B\Gamma})\boldsymbol{\vartheta}^{B\Gamma}\|^2\\ & -c_{32B}\|\tilde{\boldsymbol{r}}_1^{B\Gamma}-\tilde{\boldsymbol{r}}_d\|^2-c_{41B}\|\gamma_2\boldsymbol{G}^T\bar{\boldsymbol{\xi}}+\boldsymbol{\omega}^{B\Gamma}-\boldsymbol{\omega}_d+\gamma\Gamma\boldsymbol{\mu}^{B\Gamma}\|^2-c_{42B}\xi_1^2\|\bar{\boldsymbol{\xi}}\|^2-c_{51B}\|\boldsymbol{v}^{B\Gamma}-\boldsymbol{v}_d\|^2\\ & -c_{52B}\|\boldsymbol{\omega}^{B\Gamma}-\boldsymbol{\omega}_d\|^2+c_0,\end{aligned} \tag{66}$$

where

$$\begin{aligned}
&k_{11}=k_{11}^*-k_{11}^\diamond,\ k_{12}=k_{12}^*-k_{12}^\diamond,\ k_{12N}=k_{12N}^*-k_{12N}^\diamond\\
&k_{21}=k_{12}^\diamond-k_{12}^*,\ k_{22}=k_{22}^\diamond-k_{22}^*,\ k_{22N}=k_{22N}^\diamond-k_{22N}^*,\\
&c_0=c_0^\diamond+c_0^*+c_{0B}.
\end{aligned} \tag{67}$$

We now choose the constants ϱ, γ, γ_1, γ_2, k_{1B}, k_{2B}, $\epsilon_{ijB},(i,j)=1,2$; $\delta_{0i}, i=1,...,6$; $\delta_{1i}, i=1,2,3$; $\delta_{2i}, i=1,...,7$; $\delta_{3i}, i=1,...,7$; and $\delta_{4i}, i=1,...,4$ such that

$$\begin{aligned}
&k_{ij}\ge k_{ij}^0,\ k_{i2N}\ge k_{i2N}^0,\ (i,j)=1,2\\
&c_{ijB}\ge c_{ijB}^0,\ i=1,...,4,j=1,2,\\
&c_{i2NB}\ge c_{i2NB}^0,\ i=1,2
\end{aligned} \tag{68}$$

where k_{ij}^0, k_{i2}^0 with $(i,j)=1,2$, c_{ijB}^0 with $i=1,...,4, j=1,2$, c_{i2NB}^0 with $i=1,2$, $k_{110}^\diamond$ are positive constants.

Remark 4.3: *While the necessary conditions (68) for ensuring global practical asymptotic stability of the closed-loop system look complicated, Remark 4.4 below shows that these conditions are always feasible. The complexity of these conditions comes from the fact that the beams considered are moving and exhibit both translational and rotational large motions in addition to track a moving reference beam, for which the coupling term U_1 of the Lyapunov function U, see (36) and (37) is introduced to utilize the beam's stiffness. Strong couplings among all the motions, and between them and the reference linear and angular velocities, see Section 1 for discussion, induce the complexity in (68). Even the stabilization of beams exhibit either only small motions (vibrations) or large motions results in fairly complicated conditions to guarantee desired stability of the closed-loop system, see Do (2017a,*

2017c, 2017d, 2017e, 2018c); Do and Lucey (2018); Do and Pan (2008); He, Nie, and Meng (2017); Morgul (1992); Queiroz et al. (2000).

We elaborate the choice of the constants $\varrho_{0i}, i = 1, 2, 3$, ϱ, γ, γ_1, γ_2, k_{1B}, k_{2B}, $\epsilon_{ijB}, (i, j) = 1, 2$; $\delta_{0i}, i = 1, ..., 6$; $\delta_{1i}, i = 1, 2, 3$; $\delta_{2i}, i = 1, ..., 7$; $\delta_{3i}, i = 1, ..., 7$; and $\delta_{4i}, i = 1, ..., 4$ to ensure that the conditions listed in (43) and (68) hold in the following remark.

Remark 4.4:

1) The constant c_1: It can be seen from (42) that by choosing a small γ the inequality (43) holds for any given positive constants $\varrho_{0i}, i = 1, 2, 3$ and $0 \leq \varrho \leq 1$.

2) The constants $(k_{ij}, k_{i2N}), (i, j) = 1, 2$: If the bending stiffness is strictly larger than the shear stiffness multiplied by square of the beam's length, i.e.,

$$(EI_1 \wedge EI_2) > \Gamma^2 (G\bar{A}_1 \vee G\bar{A}_2), \tag{69}$$

then the constants $(k_{ij}, k_{i2N}), (i, j) = 1, 2$ can be made strictly positive by choosing $\varrho = 1$, see the expression of U_1 in (37); $\frac{\Gamma}{\epsilon_{16}} < \frac{2}{3}$; small $(\gamma, \epsilon_{22}, \epsilon_{23}, \epsilon_{43}$ under the conditions that $(v_{3d}^M, \bar{v}_{3d}^M, \bar{\omega}_{3d}^M)$ and $|G\bar{A}_1 - G\bar{A}_2|$ are not too large, see the expression of $k_{21}^{\diamond}$ and $k_{22}^{\diamond}$ in (60). These features usually hold for motion transporting beams because the beams are easier to be sheared than to be bent, have the same shear stiffness $G\bar{A}_1$ and $G\bar{A}_2$, and their axial velocity and acceleration, and spinning acceleration are small. If the condition (69) does not hold, the constant ϱ needs to be a small positive constant.

3) The constants $c_{ijB}, i = 1, ..., 4, j = 1, 2$ and $c_{i2NB}, i = 1, 2$: elaboration of how to ensure these constants strictly positive can be carried out similarly to the constants $(k_{ij}, k_{i2N}), (i, j) = 1, 2$.

With (68), we can write (66) as

$$\mathcal{L}U \leq -c_3 \mathcal{E} + c_0, \tag{70}$$

where

$$c_3 = k_{11} \wedge \wedge k_{12} \wedge k_{21} \wedge k_{22} \wedge k_{22N} \wedge c_{11B} \wedge c_{12B} \wedge c_{31B} \wedge c_{32B} \wedge c_{41B} \wedge c_{42B} \xi_1^2. \tag{71}$$

The control design has been completed. A block diagram of the proposed control design is depicted in Figure 2.

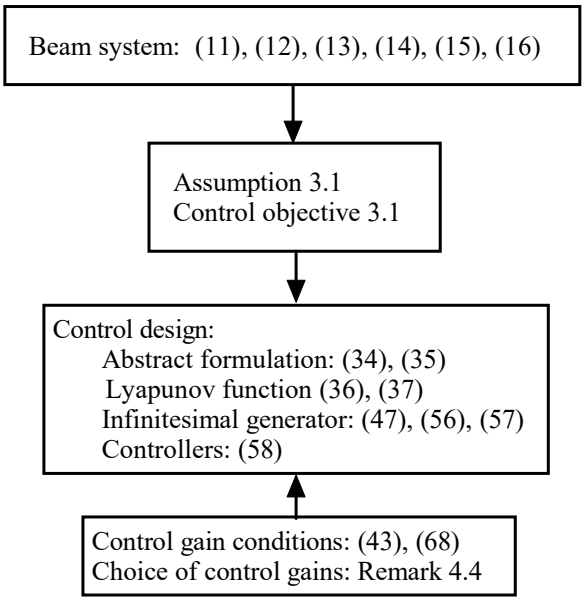

Figure 2.: Block diagram of the control design

We summarize the main results in the following theorem.

Theorem 4.1: *Under Assumption 3.1, the boundary control vectors $\boldsymbol{\phi}_{iB}, i = 1, 2$ given in (58) solve Control Objective 3.1 provided that $\varrho_{0i}, i = 1, 2, 3$, ϱ, γ, γ_1, γ_2, k_{1B}, k_{2B}, $\epsilon_{ijB}, (i, j) = 1, 2$; $\delta_{0i}, i = 1, ..., 6$; $\delta_{1i}, i = 1, 2, 3$; $\delta_{2i}, i = 1, ..., 7$; $\delta_{3i}, i = 1, ..., 7$; and $\delta_{4i}, i = 1, ..., 4$ are chosen such that the conditions in (43) and (68) hold. The closed-loop system consisting of (34), (35), and (58) is globally well-posed and globally practically asymptotically stable at the origin.*

It is noted that larger bounds on the external disturbances, see Assumption 3.1, result in a larger constant c_0 in (70), see (67) with its components in (60), (63), (65). This means that the beam tracking errors converge to a larger ball centered at the origin. However, the global practical stability is not lost due to the size of the disturbance bounds.

Proof. We first define

$$\boldsymbol{X} = \begin{bmatrix} \tilde{\boldsymbol{r}}_1 \\ \boldsymbol{q} \\ \boldsymbol{v} \\ \boldsymbol{\omega} \\ z^{B0} \\ \theta_3^{B0} \\ v_3^{B0} \\ \omega_3^{B0} \\ \tilde{\boldsymbol{r}}_1^{B\Gamma} \\ \boldsymbol{q}^{B\Gamma} \\ \tilde{\boldsymbol{r}}_2^{B\Gamma} \\ \boldsymbol{\omega}^{B\Gamma} \end{bmatrix}, \quad \boldsymbol{F}(\boldsymbol{X},t) = \begin{bmatrix} \boldsymbol{R}_1(\boldsymbol{q})\boldsymbol{v} \\ \boldsymbol{K}(\boldsymbol{q})\boldsymbol{\omega} \\ \frac{1}{m_0}\big(m_0(\boldsymbol{R}_1^{-1}(\boldsymbol{q}))_t\boldsymbol{R}_1(\boldsymbol{q})\boldsymbol{v} + \boldsymbol{R}_1^{-1}(\boldsymbol{q})\mathbb{D}\boldsymbol{n} + \boldsymbol{f}_1\big) \\ \boldsymbol{J}_0^{-1}\big(\mathbb{D}\boldsymbol{m} - \boldsymbol{\omega}\times(\boldsymbol{J}_0\boldsymbol{\omega}) + \mathbb{D}\boldsymbol{r}\times\boldsymbol{n} + \boldsymbol{f}_2\big) \\ v_3^{B0} \\ \omega_3^{B0} \\ \frac{1}{m_P}\big(N^{B0} + f_1^{B0}\big) \\ \frac{1}{J_P}\big(T^{B0} + f_2^{B0}\big) \\ \tilde{\boldsymbol{r}}_2^{B\Gamma} \\ \boldsymbol{K}(\boldsymbol{q}^{B\Gamma})\boldsymbol{\omega}^{B\Gamma} \\ \boldsymbol{M}_H^{-1}\big(-\boldsymbol{n}^{B\Gamma} + \boldsymbol{\phi}_{1B} + \boldsymbol{f}_1^{B\Gamma}\big) \\ \boldsymbol{J}_H^{-1}\big(-\boldsymbol{m}^{B\Gamma} - \boldsymbol{\omega}^{B\Gamma}\times(\boldsymbol{J}_H\boldsymbol{\omega}^{B\Gamma}) + \boldsymbol{\phi}_{2B} + \boldsymbol{f}_2^{B\Gamma}\big) \end{bmatrix} \tag{72}$$

where $\boldsymbol{\phi}_{iB}, i = 1,2$ are defined in Eq. (58). Next, we can write Eqs. (34) and (35) as follows

$$\frac{d\boldsymbol{X}}{dt} = \boldsymbol{F}(\boldsymbol{X},t). \tag{73}$$

For well-posedness and stability analysis of Eq. (73), we introduce the functional spaces: $H = (W^{1,2}(\mathcal{D}))^6\times(L^2(\mathcal{D}))^6\times\mathbb{R}^{16}$, $V = (W^{2,2}(\mathcal{D}))^6\times(L^2(\mathcal{D}))^6\times\mathbb{R}^{16}$, $V^* = (W^{-2,2}(\mathcal{D}))^6\times(L^2(\mathcal{D}))^6\times\mathbb{R}^{16}$, where $\mathcal{D} := (0,\Gamma)$, and $W^{-m,p}(\mathcal{D})$ denotes the dual of $W^{m,p}(\mathcal{D})$. Then, we have the embedding $V\subset H\equiv H^*\subset V^*$. Let

$$\hat{\boldsymbol{X}} = \mathrm{col}(\hat{\tilde{\boldsymbol{r}}}_1, \hat{\boldsymbol{q}}, \hat{\boldsymbol{v}}, \hat{\boldsymbol{\omega}}, \hat{z}^{B0}, \theta_3^{B0}, \hat{v}_3^{B0}, \hat{\omega}_3^{B0}, \hat{\tilde{\boldsymbol{r}}}_1^{B\Gamma}, \hat{\boldsymbol{q}}^{B\Gamma}, \hat{\tilde{\boldsymbol{r}}}_2^{B\Gamma}, \hat{\boldsymbol{\omega}}^{B\Gamma}). \tag{74}$$

Define

$$\begin{aligned}
\big\langle \boldsymbol{X}, \hat{\boldsymbol{X}}\big\rangle_H &= \tfrac{m_0}{2}\big\langle \boldsymbol{v}-\boldsymbol{v}_d, \hat{\boldsymbol{v}}-\boldsymbol{v}_d\big\rangle_{L^2} + \tfrac{1}{2}\big\langle \boldsymbol{\omega}-\boldsymbol{\omega}_d, \boldsymbol{J}_0(\hat{\boldsymbol{\omega}}-\boldsymbol{\omega}_d)\big\rangle_{L^2} + \tfrac{1}{2}\textstyle\sum_{i=1}^2 G\bar{A}_i\big\langle \eta_i, \hat{\eta}_i\big\rangle_{L^2} + \tfrac{EA}{2}\big\langle \varepsilon, \hat{\varepsilon}\big\rangle_{L^2} \\
&+ \tfrac{1}{2}\textstyle\sum_{i=1}^2 EI_i\big\langle \mu_i, \big(\frac{1}{2}\hat{\mu}_i - \frac{1}{6}\hat{\mu}_i^2 + \frac{1}{12}\hat{\mu}_i^3\big)\big\rangle_{L^2} + \tfrac{1}{2}\textstyle\sum_{i=1}^2 EI_i\big\langle \big(\frac{1}{2}\mu_i - \frac{1}{6}\mu_i^2 + \frac{1}{12}\mu_i^3\big), \hat{\mu}_i\big\rangle_{L^2} \\
&+ \tfrac{1}{2}GI_3\big\langle \mu_3, \big(\frac{1}{2}\hat{\mu}_3 - \frac{1}{6}\hat{\mu}_3^2 + \frac{1}{12}\hat{\mu}_3^3\big)\big\rangle_{L^2} + \tfrac{1}{2}GI_3\big\langle \big(\frac{1}{2}\mu_3 - \frac{1}{6}\mu_3^2 + \frac{1}{12}\mu_3^3\big), \hat{\mu}_3\big\rangle_{L^2} \\
&+ \tfrac{1}{2}\gamma m_0\big\langle \mathbb{D}\boldsymbol{r} - \varrho\boldsymbol{R}_1(\boldsymbol{q})\mathbb{D}\boldsymbol{r}^0, \boldsymbol{R}_1(\hat{\boldsymbol{q}})(\hat{\boldsymbol{v}}-\boldsymbol{v}_d)s\big\rangle_{L^2} + \tfrac{1}{2}\gamma m_0\big\langle \boldsymbol{R}_1(\boldsymbol{q})(\boldsymbol{v}-\boldsymbol{v}_d), \mathbb{D}\hat{\boldsymbol{r}} - \varrho\boldsymbol{R}_1(\hat{\boldsymbol{q}})\mathbb{D}\boldsymbol{r}^0 s\big\rangle_{L^2} \\
&+ \tfrac{1}{2}\gamma\big\langle \boldsymbol{\mu}, \boldsymbol{J}_0(\hat{\boldsymbol{\omega}}-\boldsymbol{\omega}_d)s\big\rangle_{L^2} + \tfrac{1}{4}\gamma\big\langle \boldsymbol{J}_0(\boldsymbol{\omega}-\boldsymbol{\omega}_d), \hat{\boldsymbol{\mu}}s\big\rangle_{L^2} + \tfrac{m_P}{2}(v_3^{B0}-v_{3d})(\hat{v}_3^{B0}-v_{3d}) \\
&+ \tfrac{J_P}{2}(\omega_3^{B0}-\omega_{3d})(\hat{\omega}_3^{B0}-\omega_{3d}) + \tfrac{1}{2}\big(\gamma_1(\tilde{\boldsymbol{r}}_1^{B\Gamma}-\tilde{\boldsymbol{r}}_d) + \boldsymbol{R}_1(\boldsymbol{q}^{B\Gamma})(\boldsymbol{v}^{B\Gamma}-\boldsymbol{v}_d) + \gamma\Gamma\boldsymbol{R}_1(\boldsymbol{q}^{B\Gamma})\boldsymbol{\vartheta}^{B\Gamma}\big)^T\boldsymbol{M}_H \\
&\times\big(\gamma_1(\hat{\tilde{\boldsymbol{r}}}_1^{B\Gamma}-\hat{\tilde{\boldsymbol{r}}}_d) + \boldsymbol{R}_1(\hat{\boldsymbol{q}}^{B\Gamma})(\hat{\boldsymbol{v}}^{B\Gamma}-\boldsymbol{v}_d) + \gamma\Gamma\boldsymbol{R}_1(\hat{\boldsymbol{q}}^{B\Gamma})\hat{\boldsymbol{\vartheta}}^{B\Gamma}\big) + \gamma_1 k_{1B}(\tilde{\boldsymbol{r}}_1^{B\Gamma}-\tilde{\boldsymbol{r}}_d)^T(\hat{\tilde{\boldsymbol{r}}}_1^{B\Gamma}-\hat{\tilde{\boldsymbol{r}}}_d) \\
&+ \tfrac{1}{2}\big(\gamma_2\boldsymbol{G}^T\bar{\boldsymbol{\xi}} + \boldsymbol{\omega}^{B\Gamma} - \boldsymbol{\omega}_d + \gamma\Gamma\boldsymbol{\mu}^{B\Gamma}\big)^T\boldsymbol{J}_H\big(\gamma_2\hat{\boldsymbol{G}}^T\hat{\bar{\boldsymbol{\xi}}} + \hat{\boldsymbol{\omega}}^{B\Gamma} - \boldsymbol{\omega}_d + \gamma\Gamma\hat{\boldsymbol{\mu}}^{B\Gamma}\big) + 2\gamma_2 k_{2B}\bar{\boldsymbol{\xi}}^T\hat{\bar{\boldsymbol{\xi}}},
\end{aligned} \tag{75}$$

where $\hat{\eta}_i, i = 1,2$, $\hat{\mu}_i, i = 1,2,3$, $\hat{\varepsilon}$, $\hat{\boldsymbol{\vartheta}}^{B\Gamma}$, $\hat{\boldsymbol{G}}$, and $\hat{\bar{\boldsymbol{\xi}}}$ are the values of $\eta_i, i = 1,2$, $\mu_i, i = 1,2,3$, ε, $\boldsymbol{\vartheta}^{B\Gamma}$, $\boldsymbol{G}$, and $\bar{\boldsymbol{\xi}}$ with $\mathbb{D}\tilde{\boldsymbol{r}}_1$ and $\boldsymbol{q}$ being replaced by $\mathbb{D}\hat{\tilde{\boldsymbol{r}}}_1$ and $\hat{\boldsymbol{q}}$, respectively. The constants $\gamma, \gamma_1, \gamma_2$, ϱ, k_{1B}, and k_{2B} the conditions specified in Theorem 4.1. Let us denote by $\big\langle \boldsymbol{X}, \hat{\boldsymbol{X}}\big\rangle_{LH}$ linearization of $\big\langle \boldsymbol{X}, \hat{\boldsymbol{X}}\big\rangle_H$ at the origin. Then, it can be verified that $\big\langle \boldsymbol{X}, \hat{\boldsymbol{X}}\big\rangle_{LH}$ is a inner product with the norm $\big\langle \boldsymbol{X}, \boldsymbol{X}\big\rangle_{LH} = \|\boldsymbol{X}\|_{LH}^2$. In fact, there exist strictly positive constants $\bar{c}_{01}$ and $\bar{c}_{02}$ such that $-\varrho_0 + \bar{c}_{01}\mathcal{E}_{LH} \le \|\boldsymbol{X}\|_{LH}^2 \le \bar{c}_{02}\mathcal{E}_{LH} + \varrho$ locally, where $\mathcal{E}_{LH}$ is the linearization of $\mathcal{E}$, which is defined in Eq. (28).

We now verify all the conditions of Theorem A.1. The continuity condition in Assumption A.1 holds due to continuity of $\boldsymbol{F}(\boldsymbol{X},t)$. By using $\big\langle \boldsymbol{X}-\hat{\boldsymbol{X}}, \boldsymbol{F}(\boldsymbol{X},t) - \boldsymbol{F}(\hat{\boldsymbol{X}},t)\big\rangle_{V,V^*} = \big\langle \boldsymbol{X}-\hat{\boldsymbol{X}}, \boldsymbol{F}(\boldsymbol{X},t) - \boldsymbol{F}(\hat{\boldsymbol{X}},t)\big\rangle_H$ with the use of the local inner product in LH defined as above and integration by parts similarly to the calculation of $\mathcal{L}U$ in Section 4.2, it is readily shown that the local monotonicity condition (A4) and local growth condition (A5) hold. From Eqs. (41) and (70), it follows that

$$\mathcal{L}U \le -\tfrac{c_3}{c_2}U + \tfrac{\varrho_0 c_3}{c_2} + c_0. \tag{76}$$

Thus, the conditions (A6), (A8) and (A9) hold. This together with Lemma 2.1 yields the proof of Theorem 4.1, i.e., the above local condition analysis, (41) and (76) (this satisfies both (A8) and (A9)) ensure both global wellposedness and global practical asymptotic stability of the closed-loop system. □

5. Simulation results

This section illustrates the effectiveness of the proposed boundary controller via some numerical simulations on an ocean drill pipe immersed in sea water. The drill pipe system parameters are taken as $\Gamma = 1000$m; outer diameter $d_o = 0.8$m; inner diameter $d_{in} = 0.4$m; $\varrho = 7850\text{kg/m}^3$; $E = 2.04 \times 10^{10}\text{kg/m}^2$; and $G = 8.4 \times 10^{10}\text{kg/m}^2$. We take $m_P = 300$kg; $J_P = 150$kg/m; $\boldsymbol{M}_H = 1000\boldsymbol{I}_3$kg; $\boldsymbol{J}_{2H} = 500\boldsymbol{I}_3$kg/m; $d_{11}^0 = 200$kg/s; $d_{21}^0 = 100\text{kgm}^2/s$; $\boldsymbol{D}_{11}^\Gamma = 500\boldsymbol{I}_3$kg/s; and $\boldsymbol{D}_{21}^\Gamma = 250\text{kgm}^2/s$. The nonlinear damping coefficients d_{22}^0 and $\boldsymbol{D}_{22}^\Gamma$ are taken to be 50% of d_{11}^0 and $\boldsymbol{D}_{21}^\Gamma$, respectively.

For the fluid loading, the one-degree-of-freedom approach in Niedzwecki and Liagre (2003), Sarpkaya and Isaacso (1981) is extended to beam motion in 3D space. This entails decomposition of the fluid motion into components perpendicular and parallel to the axis of the cylinder; the load due to the former is obtained from bluff-body analysis while the load due to the latter arises from the effect of skin-friction and is modeled using boundary-layer theory. The resulting expressions for $\boldsymbol{D}_{11} = \text{diag}(d_{111}, d_{112}, d_{113})$ and $\boldsymbol{D}_{21} = \text{diag}(d_{211}, d_{212}, d_{213})$ are derived as follows:

$$d_{k1i} = C_{Lki} + C_{Dki}\frac{\varrho_w d_o}{2}\sqrt{\frac{8}{\pi}}\sigma_{ki}(s,t), \tag{77}$$

for $k = 1, 2$ and $i = 1, 2, 3$, where ϱ_w is the sea water density; C_{Li} are the (structural) linear viscous damping coefficients; C_{Di} are the skin-friction drag coefficients; and $\sigma_i(s,t)$ is the root mean square of the water particle velocity. The nonlinear damping coefficient matrix $\boldsymbol{D}_{22}$ taken to be 50% of $\boldsymbol{D}_{21}$. The coefficients of distributed damping and fluid loads are taken as $C_{L11} = C_{L12} = 120\frac{\text{Ns}}{\text{m}}$, $C_{L13} = 60$Ns, $C_{D11} = C_{D12} = 1.2$, $C_{D13} = 0.6$; $C_{L21} = C_{L22} = 90$Ns, $C_{L23} = 60$Nms, $C_{D21} = C_{D22} = 0.8$, $C_{D23} = 0.4$; and sea-water density is $\varrho_w = 1025\text{kg/m}^3$. Using linear wave theory, the water particle velocities ϑ_i are Niedzwecki and Liagre (2003):

$$\vartheta_i(z,t) = \sum_{j=1}^{N_i} A_{ij}\omega_{ij}\frac{\cosh(k_{ij}z)}{\sinh(k_{ij}L)}\sin(\omega_{ij}t + \xi_{ij}), \tag{78}$$

where $\xi_{ij} = 2\pi\text{rand}()$ with rand() being a random number between 0 and 1, the amplitude A_{ij}, wave number k_{ij}, and frequency ω_{ij} of the wave j^{th} are given by

$$\begin{aligned} &\omega_{ij} = \omega_{im} + \frac{\omega_{iM} - \omega_{im}}{N_i}j,\ S_{ij} = \frac{1.25}{4}\frac{\omega_{io}^4}{\omega_j^5}H_i^2 e^{-1.25\left(\frac{\omega_{io}}{\omega_j}\right)^4} \\ &A_{ij} = \sqrt{2S_{ij}\frac{\omega_{iM} - \omega_{im}}{N_i}},\ 9.8k_{ij}\tanh(k_{ij}\Gamma) = \omega_{ij}^2. \end{aligned} \tag{79}$$

In (79), the minimum and maximum wave frequencies are $\omega_{im} = 0.2$rad/s, $\omega_{iM} = 2.5$rad/s; the two-parameter Bretschneider spectrum S_{ij} are used with the significant wave heights $H_i = 4$m; the modal frequency is $\omega_{io} = \frac{2\pi}{T_i}$ with the period $T_1 = T_2 = 7.8$, $T_3 = 5$; $N_i = 10$.

The initial conditions are taken as $t_0 = 0$; $\tilde{\boldsymbol{r}}_{10}(s) = \text{col}(4\sin\left(\frac{4\pi}{\Gamma}s\right), -4\sin\left(\frac{4\pi}{\Gamma}s\right), -0.75\sin\left(\frac{2\pi}{\Gamma}s\right))$; $\tilde{\boldsymbol{r}}_{20}(s) = 0$; $\boldsymbol{\theta}_0(s) = \text{col}\big(0.6\sin\left(\frac{6\pi}{\Gamma}s\right), 0.75\cos\left(\frac{6\pi}{\Gamma}s\right), 1.5\sin\left(\frac{4\pi}{\Gamma}s\right)\big)$; and $\boldsymbol{\omega}_0(s) = 0$. The reference velocities are taken as $v_{3d} = 0.1$m/s and $\omega_{3d} = 20$rad/s. Following Remark 4.4, the control gains are chosen as follows: $\varrho = 0.05$, $\gamma = \frac{1}{100\Gamma}$, $\gamma_1 = \gamma_2 = 3.5\gamma\Gamma$, $k_{1B} = 5EA$, $k_{2B} = 5EI$, $\epsilon_{1iB} = \frac{1}{2}EA, i = 1, 2$, and $\epsilon_{2iB} = \frac{1}{2}EI, i = 1, 2$. It is readily checked that the above choice of the control gains ensures that all the conditions specified in Theorem 4.1 hold for some positive constants $\varrho_{0i}, i = 1, 2, 3$, $\delta_{0i}, i = 1, ..., 6$; $\delta_{1i}, i = 1, 2, 3$; $\delta_{2i}, i = 1, ..., 7$; $\delta_{3i}, i = 1, ..., 7$; and $\delta_{4i}, i = 1, ..., 4$.

We run two simulations. In the first simulation, the control in Do (2017c), see (57) in this reference, with the vectors $\tilde{\boldsymbol{r}}_1^{B\Gamma}$, $\tilde{\boldsymbol{r}}_2^{B\Gamma}$, $\boldsymbol{\theta}^{B\Gamma}$, and $\boldsymbol{\omega}^{B\Gamma}$ being substituted by $\tilde{\boldsymbol{r}}_1^{B\Gamma} = \tilde{\boldsymbol{r}}_1^{B\Gamma} - \boldsymbol{r}_d$, $\tilde{\boldsymbol{r}}_2^{B\Gamma} = \tilde{\boldsymbol{r}}_2^{B\Gamma} - \boldsymbol{v}_d$, $\boldsymbol{\theta}^{B\Gamma} = \boldsymbol{\theta}^{B\Gamma} - \text{col}(\theta_1^{B\Gamma}, \theta_2^{B\Gamma}, \theta_3^{B\Gamma} - \omega_{3d}(t - t_0))$, and $\boldsymbol{\omega}^{B\Gamma} = \boldsymbol{\omega}^{B\Gamma} - \boldsymbol{\omega}_d$, respectively, to make the stabilization control in Do (2017c) become a velocity tracking one. The control gains are taken the same as those in the simulation in Do (2017c). In the second simulation, the proposed boundary controls (58) is used. In both simulations, the length of simulation time is 500 seconds. Moreover, the second order (in space and time) centered, implicit finite difference scheme is used to numerically solve the partial differential equations (4) plus the boundary conditions (15) where the boundary controls $\phi_{iB}, i = 1, 2, 3$ given in (58). The time step is $\Delta t = 0.01$ and space step is $\Delta z = 0.2$. This choice ensures that the convergence parameter $r = \frac{\Delta t}{(\Delta z)^2} = 0.25$ is positive and less than 0.5 as required for stable solutions Smith (1985). If the discretized steps are too large, the numerical solution will be unstable. If they are too small (provided they satisfy the above condition), simulation time will be very long.

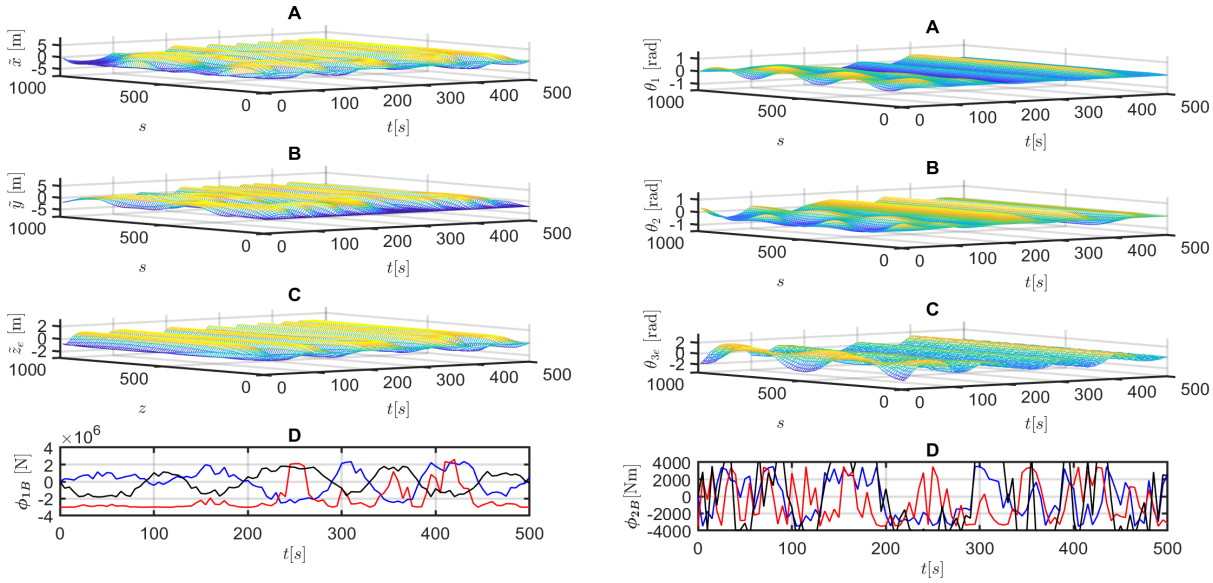

a) Translational displacements and boundary control ϕ_{1B}.

b) Rotational angles and boundary control ϕ_{2B}.

Figure 3.: Simulation results with the control design in Do (2017c)

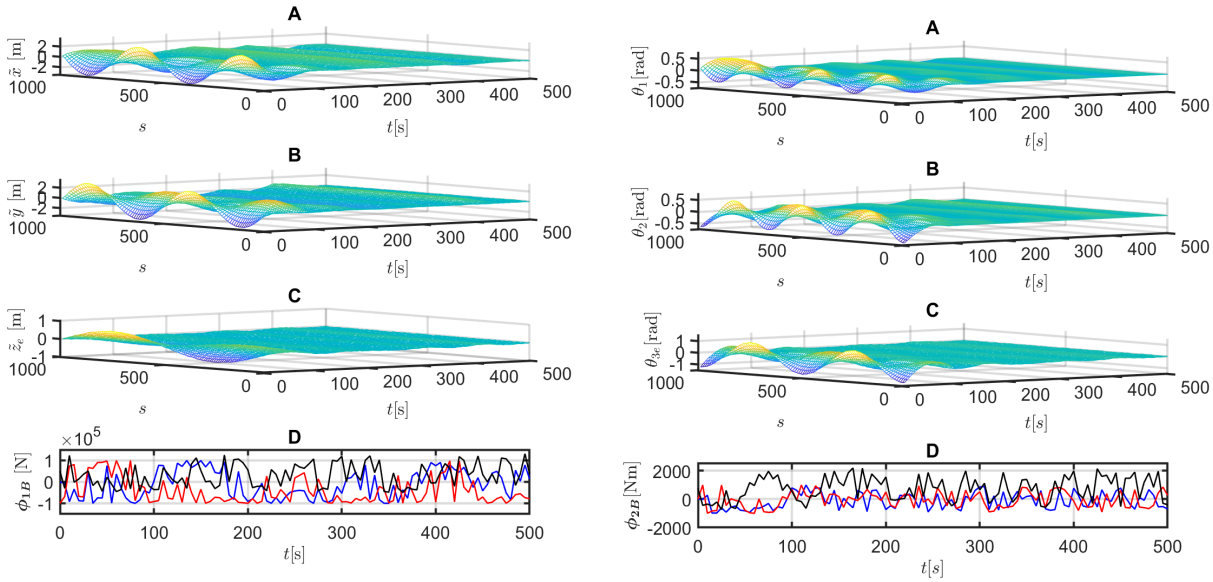

a) Translational displacements and boundary control ϕ_{1B}.

b) Rotational angles and boundary control ϕ_{2B}.

Figure 4.: Simulation results with the proposed boundary controls

Case of the control in Do (2017c): The results are plotted in Figure 3a and Figure 3b. The displacements $(\tilde{x}(s,t), \tilde{y}(s,t), \tilde{z}_e(s,t))$, where $\tilde{z}_e(s,t) = \tilde{z}(s,t) - z_d$ with $\dot{z}_d = v_{3d}$ and $z_d(0) = 0$, are plotted in Sub-figures. 3a.A, 3a.B and 3a.C, the rotations $(\theta_1(s,t), \theta_2(s,t), \theta_{3e}(s,t))$, where $\theta_{3e}(s,t) = \theta_3(s,t) - \theta_d(t)$ with $\dot{\theta}_{3d} = \omega_{3d}$ and $\theta_d(0) = 0$, are plotted in Sub-figures 3b.A, 3b.B and 3b.C, while the controls ϕ_{1B} and ϕ_{2B} are plotted in Sub-figure 3a.D and Sub-figure 3b.D. It is seen that the displacements and rotations oscillate within a ball centered at the origin with a quite large radius due to the sea loads and axial and rotational motions. This is due to the robustness property of the control in Do (2017c), which is a nice property of the Lyapunov-based control design Khalil (2002); Krstic et al. (1995).

Case with the proposed feedbacks (58): The results are plotted in Figure4a and Figure 4b.

Comparing Sub-figure. (4a.A, 4a.B, 4a.C, 4b.A, 4b.B, 4b.C) in this case with corresponding Sub-figures (3a.A, 4a.B, 3a.C, 3b.A, 3b.B, 3b.C) in the case, where the control design in Do (2017c) is used, clearly shows an excellent performance of the proposed controller in the sense of a large reduction (about 5 times less) in magnitude of all displacements and rotations. This is because as mentioned before the control design in Do (2017c) is for stabilization, where the couplings of the reference velocities with all other motions are not considered in the control design. It is also observed from Sub-figures (3a.D, 3b.D) and Sub-figures. (4a.D, 4b.D) that the controls $\boldsymbol{\phi}_{1B}$ and $\boldsymbol{\phi}_{2B}$ corresponding to the control design in Do (2017c) are larger than those in the present paper because all the motions with the controls in Do (2017c) have larger magnitudes than those in the present paper. Note that if the external disturbances increase, the radius of the ball centered at the origin will be larger, see the discussion just below Theorem 4.1, and of course the control efforts will become larger.

6. Conclusions

The problem for beams to track reference axial and rotational velocities in space was posed and boundary controllers were designed to stabilize them at their reference states. In the control design and analysis of well-posedness and stability, exact nonlinear partial differential equations governing motion of the beams were used. Various tools including coordinate transformations, Sobolev embeddings, and a Lyapunov-type theorem developed for a class of evolution systems in Hilbert space were utilized to handle difficulties caused by large motion couplings of the beams in space. Future work is to consider the boundary control problem for a group of beams.

Appendix A. Well-posedness and Stability of Nonlinear Evolution Systems

This appendix presents results on well-posedness (existence, uniqueness, and continuous dependence on initial conditions) and stability of nonlinear evolution systems. These results are used in control design and stability analysis of the beam system.

A.1. *Space notations*

Let H be a separable Hilbert space identified with its dual H^* by the Riesz isomorphism. Let V be a real reflexible Banach space such that $V \subset H$ continuously and densely, and V^* be the dual of V. From the definitions of H and V, we have that the embedding $V \subset H \equiv H^* \subset V^*$ is continuous and dense. We denote by $\|.\|_H$, $\|.\|_V$, and $\|.\|_{V^*}$ the norms in H, V, and V^*, respectively; by $\langle .,. \rangle_{V,V^*}$ (i.e., $\langle \boldsymbol{z}, \boldsymbol{v} \rangle_{V,V^*} = \boldsymbol{z}(\boldsymbol{v})$ for $\boldsymbol{z} \in V^*, \boldsymbol{v} \in V$) the duality product between V and V^*; and by $\langle .,. \rangle_H$ the inner product in H. The duality product between V and V^* has the following property Gawarecki and Mandrekar (2011):

$$\langle \boldsymbol{u}, \boldsymbol{v} \rangle_{V,V^*} = \langle \boldsymbol{u}, \boldsymbol{v} \rangle_H, \boldsymbol{u} \in H, \boldsymbol{v} \in V. \tag{A1}$$

A.2. *Evolution systems*

Let us consider the nonlinear evolution system on the space H:

$$\frac{d\boldsymbol{X}(t)}{dt} = \boldsymbol{F}(\boldsymbol{X}(t), t), \ \boldsymbol{X}(t_0) = \boldsymbol{X}_0 \in H, \tag{A2}$$

where $\boldsymbol{X}$ is assumed to be in H for almost every (a.e.) $t \in [t_0, \infty)$ and $\boldsymbol{F} : H \times [t_0, \infty) \to V^*$ is a family of nonlinear operators defined for a.e. $t \in [t_0, \infty)$. The following definition is a deterministic version of the stochastic one in (Chow, 2007).

Definition A.1: *A H-valued process $\{\boldsymbol{X}(t), t \in [t_0, T]\}$ is said to be a variational solution of (A2) if for any $\boldsymbol{\psi} \in V$:*

$$\langle \boldsymbol{X}(t), \boldsymbol{\psi} \rangle_H = \langle \boldsymbol{X}_0, \boldsymbol{\psi} \rangle_H + \int_{t_0}^{t} \langle \boldsymbol{F}(\boldsymbol{X}(s), s), \boldsymbol{\psi} \rangle_{V,V^*} ds \tag{A3}$$

for each $t \in [t_0, T]$. If T is replaced by ∞, then $\boldsymbol{X}(t), t \geq t_0$, is said to be a global variational solution of (A2).

The following definition is an extended version of the one in finite dimensional space in (Khalil, 2002) to infinite dimensional space.

Definition A.2: *The variational solution of (A2) is said to be*

(1) globally stable if, for each $\boldsymbol{X}_0 \in H$*, there exists* $\delta = \delta(\|\boldsymbol{X}_0\|_H)$ *such that* $\|\boldsymbol{X}(t)\|_H \leq \delta(\|\boldsymbol{X}_0\|_H)$*, a.e.* $(\boldsymbol{X}, t) \in V \times [t_0, \infty)$*;*

(2) globally exponentially stable if it is globally stable and $\|\boldsymbol{X}(t)\|_H \leq \|\boldsymbol{X}(t_0)\|_H e^{-c(t-t_0)}$*, a. e.* $(\boldsymbol{X}, t) \in V \times [t_0, \infty)$*, where* c *is a positive constant;*

(3) globally practically exponentially stable if it is globally stable and $\|\boldsymbol{X}(t)\|_H \leq \|\boldsymbol{X}(t_0)\|_H e^{-c(t-t_0)} + c_0$*, a.e.* $(\boldsymbol{X}, t) \in V \times [t_0, \infty)$*, where* c *is a positive constant, and* c_0 *is positive constant.*

If c *depends on the initial condition, then "exponentially" is replaced by "asymptotically" in the above statements.*

A.3. *Well-posedness and stability of evolution systems*

We assume that $\boldsymbol{F} : H \times [t_0, \infty) \to V^*$ is measurable and satisfies the following continuity and local monotonicity and growth conditions.

Assumption A.1:

1) [Continuity] The mapping $V \ni \boldsymbol{v} \to \boldsymbol{F}(\boldsymbol{v}, t) \in V^*$ *is continuous a.e.* $t \in [t_0, \infty)$*.*

2) [Local monotonicity] For any $\boldsymbol{u}, \boldsymbol{v} \in V$ *with* $\|\boldsymbol{u}\|_H \leq \epsilon$ *and* $\|\boldsymbol{v}\|_H \leq \epsilon$*, where* ϵ *is a positive constant, there exists a constant* c_ϵ *such that*

$$2\big\langle \boldsymbol{u} - \boldsymbol{v}, \boldsymbol{F}(\boldsymbol{u}, t) - \boldsymbol{F}(\boldsymbol{v}, t)\big\rangle_{V,V^*} \leq c_\epsilon \|\boldsymbol{u} - \boldsymbol{v}\|_H^2, \tag{A4}$$

a.e. $t \in [t_0, \infty)$*.*

3) [Local growth] There exists a constant δ *such that:*

$$\|\boldsymbol{F}(\boldsymbol{u}, t)\|_{V^*} \leq \delta(1 + \|\boldsymbol{u}\|_V^{p-1}) \; \forall \, \boldsymbol{u} \in V, \|\boldsymbol{u}\|_V \leq \epsilon. \tag{A5}$$

Theorem A.1: *Under Assumption A.1, suppose that there exist a function* $U(\boldsymbol{X}, t) \in C^1(H; [t_0, \infty))$ *referred to as a Lyapunov function, an integer* $p \geq 0$*, and nonnegative constants* ϱ_1 *and* ϱ_2 *such that*

$$-\varrho_1 + \|\boldsymbol{X}\|_H^p \leq U(\boldsymbol{X}, t) \leq \|\boldsymbol{X}\|_H^p + \varrho_2, \tag{A6}$$

a.e. $(\boldsymbol{X}, t) \in V \times [t_0, \infty)$*, and that the generator* $\mathcal{L}U := \frac{dU}{dt}$ *given by*

$$\mathcal{L}U(\boldsymbol{X}, t) = U_t(\boldsymbol{X}, t) + \big\langle \boldsymbol{F}(\boldsymbol{X}, t), U_{\boldsymbol{X}}(\boldsymbol{X}, t)\big\rangle_{V,V^*}, \tag{A7}$$

with $U_t(\boldsymbol{X}, t)$ *and* $U_{\boldsymbol{X}}(\boldsymbol{X}, t)$ *being the (Fréchet) derivatives of* $U(\boldsymbol{X}, t)$ *with respect to* t *and* $\boldsymbol{X}$*, respectively.*

1) [well-posedness] If the generator $\mathcal{L}U(\boldsymbol{X}, t)$ *satisfies*

$$\mathcal{L}U(\boldsymbol{X}, t) \leq c(1 + U(\boldsymbol{X}, t)), \;\; a.e. \; (\boldsymbol{X}, t) \in V \times [t_0, \infty), \tag{A8}$$

where c *is a nonnegative constant. Then the system (A2) is globally well-posed in terms of the variational solution for each* $\boldsymbol{X}_0 \in H$*.*

2) [stability] If the generator $\mathcal{L}U(\boldsymbol{X}, t)$ *satisfies*

$$\mathcal{L}U(\boldsymbol{X}, t) \leq -c_3 \|\boldsymbol{X}\|_H^p + c_0, \;\; a.e. \; (\boldsymbol{X}, t) \in V \times [t_0, \infty), \tag{A9}$$

where c_3 *is a positive constant. If* $c_0 = 0$*,* $\varrho_1 = 0$*, and* $\varrho_2 = 0$*, the equilibrium* $\boldsymbol{X} \equiv 0$ *is globally exponentially stable. If any of* c_0*,* ϱ_1*, and* ϱ_2 *is a positive constant, the equilibrium* $\boldsymbol{X} \equiv 0$ *is globally practically exponentially stable. Moreover, if* c_3 *depends on the initial condition, then "exponentially" is replaced by "asymptotically" in the above statements.*

Proof. See Do (2018a).

References

Adams, R. A., & Fournier, J. J. F. (2003). *Sobolev spaces* (2nd ed.). Oxford, UK: Academic Press.

AliExpress. (2020). `https://www.aliexpress.com/i/32968741696.html`, Accessed: 12-03-2020.

Chow, P. L. (2007). *Stochastic partial differential equations.* Boca Raton: Chapman & Hall/CRC.

Do, K. D. (2015). Coordination control of quadrotor VTOL aircraft in three dimensional space. *International Journal of Control*, *88*(3), 543-558.

Do, K. D. (2016). Stability of nonlinear stochastic distributed parameter systems and its applications. *Journal of Dynamic Systems, Measurement, and Control*, *138*, 101010-1:101010-12.

Do, K. D. (2017a). Boundary control design for extensible marine risers in three dimensional space. *Journal of Sound and Vibration*, *388*, 1-19.

Do, K. D. (2017b). Boundary control of slender beams under deterministic and stochastic loads. *Journal of Dynamic Systems, Measurement, and Control*, *139*, 091012-1:091012-14.

Do, K. D. (2017c). Modeling and boundary control of translational and rotational motions of nonlinear slender beams in three-dimensional space. *Journal of Sound and Vibration*, *389*, 1-23.

Do, K. D. (2017d). Stochastic boundary control design for extensible marine risers in three dimensional space. *Automatica*, *77*, 184-197.

Do, K. D. (2017e). Stochastic boundary control design for Timoshenko beams with large motions. *Journal of Sound and Vibration*, *402*, 164-184.

Do, K. D. (2018a). Modeling and boundary control of slender curved beams. *International Journal of Control*, *91*, 1873-1895.

Do, K. D. (2018b). Stabilisation of large motions of Euler-Bernoulli beams by boundary controls. *International Journal of Systems Science*, *49*, 736-754.

Do, K. D. (2018c). Stabilization of exact nonlinear Timoshenko beams in space by boundary feedback. *Journal of Sound and Vibration*, *422*, 278-299.

Do, K. D., & Lucey, A. D. (2017). Boundary stabilization of extensible and unshearable marine risers with large in-plane deflection. *Automatica*, *77*, 279-292.

Do, K. D., & Lucey, A. D. (2018). Stochastic stabilization of slender beams in space: Modeling and boundary control. *Automatica*, *91*, 279-293.

Do, K. D., & Pan, J. (2008). Boundary control of transverse motion of marine risers with actuator dynamics. *Journal of Sound and Vibration*, *318*(4-5), 768-791.

Do, K. D., & Pan, J. (2009). Boundary control of three-dimensional inextensible marine risers. *Journal of Sound and Vibration*, *327*(3-5), 299-321.

Dong, G., & Chen, P. (2016). A review of the evaluation, control, and application technologies for drill string vibrations and shocks in oil and gas well. *Shock and Vibration*, *2016*, 1-34.

Endo, T., Matsuno, F., & Jia, Y. (2017). Boundary cooperative control by flexible Timoshenko arms. *Automatica*, *81*, 377-389.

Gawarecki, L., & Mandrekar, V. (2011). *Stochastic differential equations in infinite dimensions with applications to stochastic partial differential equations*. Berlin: Springer.

He, W., Ge, S. S., & C.Liu. (2014). Adaptive boundary control for a class of inhomogeneous Timoshenko beam equations with constraints. *IET Control Theory & Applications*, *8*, 1285-1292.

He, W., Huang, T. M. D., & Li, X. (2017). Adaptive boundary iterative learning control for an euler-bernoulli beam system with input constraint. *IEEE Transactions on Neural Networks and Learning Systems, In press*.

He, W., Meng, T., He, X., & Ge, S. S. (2018). Unified iterative learning control for flexible structures with input constraints. *Automatica*, *96*, 326-336.

He, W., Meng, T., Liu, J. K., & Qin, H. (2015). Boundary control of a Timoshenko beam system with input dead-zone. *International Journal of Control*, *88*, 1257-1270.

He, W., Nie, S., & Meng, T. (2017). Modeling and vibration control for a moving beam with application in a drilling riser. *IEEE Transactions on Control Systems Technology*, *25*, 1036-1043.

Khalil, H. (2002). *Nonlinear systems*. Prentice Hall.

Kim, J. U., & Renardy, Y. (1987). Boundary control of the Timoshenko beam. *SIAM Journal of Control and Optimization*, *25*, 1417-1429.

Krstic, M., Kanellakopoulos, I., & Kokotovic, P. (1995). *Nonlinear and adaptive control design*. New York: Wiley.

Krstic, M., Siranosian, A. A., & Smyshlyaev, A. A. (2006). Backstepping boundary controllers and observers for the slender Timoshenko beam: Part i control design. *In 45th IEEE Conference on Decision and Control, San Diego, CA*, 3938-3943.

Krstic, M., Siranosian, A. A., Smyshlyaev, A. A., & Bement, M. (2006). Backstepping boundary controllers and observers for the slender Timoshenko beam: Part ii stability and simulations. *In American Control Conference, Minneapolis, MN*, 2412-2417.

Krstic, M., & Smyshlyaev, A. (2008). *Boundary control of pdes: A course on backstepping designs*. Philadelphia, PA: Society for Industrial and Applied Mathematics.

Kuipers, J. B. (2002). *Quaternions and rotation sequences: A primer with applications to orbits, aerospace and virtual reality*. New Jersey: Princeton University Press.

Liu, Y., Zhao, Z., & He, W. (2016a). Boundary control of an axially moving accelerated/decelerated belt system. *International Journal of Robust and Nonlinear Control*, *26*, 3849-3866.

Liu, Y., Zhao, Z., & He, W. (2016b). Stabilization of an axially moving accelerated/decelerated system via an adaptive boundary control. *ISA Transactions*, *64*, 394-404.

Liu, Y., Zhao, Z., & He, W. (2017). Boundary control of an axially moving system with high acceleration/deceleration and disturbance observer. *Journal of the Franklin Institute*, *354*, 2905-2923.

Manjunath, T. C., & Bandyopadhyay, B. (2009). Vibration control of Timoshenko smart structures using multirate outputfeedback based discrete sliding mode control for SISO systems. *Journal of Soundand Vibration*, *326*, 50-74.

Mei, C. (2009). Hybrid wave/mode active control of bending vibrations in beams based on the advanced Timoshenko theory. *Journal of Soundand Vibration*, *322*, 29-38.

Morgul, O. (1992). Dynamic boundary control of the Timoshenko beam. *Automatica*, *28*, 1255-1260.

Niedzwecki, J. M., & Liagre, P. Y. F. (2003). System identification of distributed-parameter marine riser models. *Ocean Engineering*, *30*(11), 1387-1415.

Orthwein, W. C. (1968). A nonlinear stress-strain relation. *International Journal of Solids and Structures*, *4*, 371-382.

Queiroz, M. S. D., Dawson, M., Nagarkatti, S., & Zhang, F. (2000). *Lyapunov-based control of mechanical systems*. Boston: Birkhauser.

Sarpkaya, T., & Isaacso, M. (1981). *Mechanics of wave forces on offshore structures*. New York: Van Nostrand Reinhold.

Smith, G. D. (1985). *Numerical solutions of partial differential equations: Finite difference methods* (3rd ed.). Oxford: Clarendon Press.

Tabarrok, B., Leech, C. M., & Kim, Y. I. (1974). On the dynamics of axially moving beams. *Journal of the Franklin Institute*, *297*, 201-220.

Tucker, R. W., & Wang, C. (2003). Torsional vibration control and cosserat dynamics of a drill-rig assembly. *Meccanica*, *38*.

Xu, G., & Wang, H. (2013). Stabilisation of Timoshenko beam system with delay in the boundary control. *International Journal of Control*, *86*, 1165-1178.

Yang, K. J., Hong, K. S., & Matsuno, F. (2005). Energy-based control of axially translating beams: Varying tension, varying speed, and disturbance adaptation. *IEEE Transactions on Control Systems Technology*, *13*, 1045-1054.